
Improved uniform error bounds for the time-splitting methods for the long-time dynamics of the Schrödinger/nonlinear Schrödinger equation

Weizhu Bao · Yongyong Cai · Yue Feng

Received: date / Accepted: date

Abstract We establish improved uniform error bounds for the time-splitting methods for the long-time dynamics of the Schrödinger equation with small potential and the nonlinear Schrödinger equation (NLSE) with weak nonlinearity. For the Schrödinger equation with small potential characterized by a dimensionless parameter $\varepsilon \in (0, 1]$ representing the amplitude of the potential, we employ the unitary flow property of the (second-order) time-splitting Fourier pseudospectral (TSFP) method in L^2 -norm to prove a uniform error bound at $C(T)(h^m + \tau^2)$ up to the long time $T_\varepsilon = T/\varepsilon$ for any $T > 0$ and uniformly for $0 < \varepsilon \leq 1$, while h is the mesh size, τ is the time step, $m \geq 2$ depends on the regularity of the exact solution, and $C(T) = C_0 + C_1T$ grows at most linearly with respect to T with C_0 and C_1 two positive constants independent of T , ε , h and τ . Then by introducing a new technique of *regularity compensation oscillation* (RCO) in which the high frequency modes are controlled by regularity and the low frequency modes are analyzed by phase cancellation and energy method, an improved uniform error bound at $O(h^{m-1} + \varepsilon\tau^2)$ is established in H^1 -norm for the long-time dynamics up to the time at $O(1/\varepsilon)$ of the Schrödinger equation with $O(\varepsilon)$ -potential with $m \geq 3$, which is uniformly for $\varepsilon \in (0, 1]$. Moreover, the RCO technique is extended to prove an improved uniform error bound at $O(h^{m-1} + \varepsilon^2\tau^2)$ in H^1 -norm for the long-time dynamics up to the time at $O(1/\varepsilon^2)$ of the cubic NLSE with $O(\varepsilon^2)$ -nonlinearity strength, uniformly for $\varepsilon \in (0, 1]$ as a dimensionless parameter. Extensions to the first-order and fourth-order time-splitting methods are discussed. Numerical results are reported to validate our error estimates and to demonstrate that they are sharp.

W. Bao

Department of Mathematics, National University of Singapore, Singapore 119076
E-mail: matbaowz@nus.edu.sg

Y. Cai

Laboratory of Mathematics and Complex Systems and School of Mathematical Sciences, Beijing Normal University, Beijing 100875, China
E-mail: yongyong.cai@bnu.edu.cn

Y. Feng

Department of Mathematics, National University of Singapore, Singapore 119076
E-mail: fengyue@u.nus.edu

Keywords Schrödinger equation · nonlinear Schrödinger equation · long-time dynamics · time-splitting Fourier pseudospectral method · improved uniform error bound · regularity compensation oscillation (RCO)

1 Introduction

The (nonlinear) Schrödinger equation arises in various physical phenomena, such as quantum mechanics, Bose-Einstein condensates, laser beam propagation, plasma and particle physics [2, 14, 23, 24, 38]. In this paper, we consider the following Schrödinger equation

$$i\partial_t\psi(\mathbf{x}, t) = -\Delta\psi(\mathbf{x}, t) + \varepsilon V(\mathbf{x})\psi(\mathbf{x}, t), \quad \mathbf{x} \in \Omega, \quad t > 0, \quad (1.1)$$

and the nonlinear Schrödinger equation (NLSE)

$$i\partial_t\psi(\mathbf{x}, t) = -\Delta\psi(\mathbf{x}, t) \pm \varepsilon^2|\psi(\mathbf{x}, t)|^2\psi(\mathbf{x}, t), \quad \mathbf{x} \in \Omega, \quad t > 0, \quad (1.2)$$

with the initial data

$$\psi(\mathbf{x}, 0) = \psi_0(\mathbf{x}), \quad \mathbf{x} \in \overline{\Omega}, \quad (1.3)$$

where $\Omega = \prod_{i=1}^d(a_i, b_i) \subset \mathbb{R}^d$ is a bounded domain equipped with periodic boundary conditions. Here, t is time, $\mathbf{x} = (x_1, \dots, x_d)^T \in \mathbb{R}^d$ ($d = 1, 2, 3$) is the spatial coordinate, $\psi(\mathbf{x}, t) \in \mathbb{C}$ is the complex order parameter/wave function, $V(\mathbf{x}) \in \mathbb{R}$ is a given external potential, $\varepsilon \in (0, 1]$ is a dimensionless parameter. In the Schrödinger equation (1.1), the amplitude of the potential is characterized by the parameter $\varepsilon \in (0, 1]$. In the NLSE (1.2), the strength of the nonlinearity is $O(\varepsilon^2)$ – *NLSE with weak nonlinearity* – and the dynamics of the NLSE (1.2) with $O(1)$ -initial data is equivalent to the NLSE with $O(1)$ -nonlinearity and $O(\varepsilon)$ -initial data – *NLSE with small initial data*, e.g. by setting $\phi(\mathbf{x}, t) = \varepsilon\psi(\mathbf{x}, t)$, the NLSE (1.2) with (1.3) becomes

$$\begin{cases} i\partial_t\phi(\mathbf{x}, t) = -\Delta\phi(\mathbf{x}, t) \pm |\phi(\mathbf{x}, t)|^2\phi(\mathbf{x}, t), & \mathbf{x} \in \Omega, \quad t > 0, \\ \phi(\mathbf{x}, 0) = \varepsilon\psi_0(\mathbf{x}) := \phi_0(\mathbf{x}) = O(\varepsilon), & \mathbf{x} \in \overline{\Omega}. \end{cases} \quad (1.4)$$

In the past two decades, many accurate and efficient numerical methods have been proposed and analyzed to simulate the (nonlinear) Schrödinger equation including the finite difference time domain (FDTD) methods [1, 3, 21], the exponential wave integrator Fourier pseudospectral (EWI-FP) method [15, 32], the time-splitting Fourier pseudospectral (TSFP) method [8, 5, 34, 42], etc. Among these numerical methods, the TSFP method preserves a set of geometric properties and performs much better than the other numerical approaches regarding the stability, efficiency, accuracy and spatial/temporal resolution [2, 5, 6]. However, convergence analysis for the TSFP method applied to the (nonlinear) Schrödinger equation is normally valid up to the finite-time dynamics at $O(1)$ and we refer to [5, 8, 24, 30, 34, 41] and references therein.

Recently, long-time behaviors of the (nonlinear) Schrödinger equation on compact domains have received a great deal of attention [10, 13, 24, 25, 26]. Along the analytical front, the existence of the solution, the asymptotic behavior and conservation laws have been well studied in the literature [9, 11, 20, 31, 39]. From the viewpoint of numerical analysis, the stability of the plane wave solutions and

long-time preservations of the actions and energy for the TSFP method have been shown for the NLSE with the help of Birkhoff normal form and the modulated Fourier expansion [19, 26, 27, 28, 29]. For the long-time error estimates of the numerical schemes, improved error bounds for time-splitting methods have been proven under the constraint that the time step τ is an integer fraction of the period of the principal linear part [16]. Due to the usage of the properties for the periodic function, extensions of the improved error bounds to higher dimensions require that the aspect ratio of the domain is rational. In addition, error estimates of the splitting methods applied to Maxwell's equations have been established with the error bound growing linearly in time [17, 18]. However, such linear growth of the TSFP error bound for the Schrödinger equation has not been reported.

The aim of this work is to establish the improved uniform error bounds for the TSFP method for the long-time dynamics of the Schrödinger equation with small potential and the NLSE with weak nonlinearity. First, we prove a uniform error bound in L^2 -norm for the TSFP method applied to the Schrödinger equation with the constant in the error bound growing linearly with respect to the time T . Based on this error bound, for a given accuracy tolerance δ_0 and time step τ , we could obtain the computational time within the accuracy δ_0 by using the TSFP method is $O(\delta_0/\tau^2)$ for $\varepsilon = 1$, i.e., with the smaller time step τ , the longer dynamics for the Schrödinger equation can be calculated! Then by introducing a new technique of **regularity compensation oscillation** (RCO) in which the high frequency modes are controlled by regularity and the low frequency modes are analyzed by phase cancellation and energy method, an improved uniform error bound in H^1 -norm for the Schrödinger equation with $O(\varepsilon)$ -potential up to the time $O(1/\varepsilon)$ is carried out at $O(h^{m-1} + \varepsilon\tau^2 + \tau_0^{m-1})$ with $m \geq 3$ depending on the regularity of the exact solution and $\tau_0 \in (0, 1)$ a parameter fixed. In addition, the technique of RCO is extended to the proof of an improved uniform error bound for the cubic NLSE with $O(\varepsilon^2)$ -nonlinearity strength up to the time at $O(1/\varepsilon^2)$ with the error bound in H^1 -norm at $O(h^{m-1} + \varepsilon^2\tau^2 + \tau_0^{m-1})$.

Here, we briefly explain the idea of our analysis. For sufficiently regular solution, we use the smoothness of the exact solution to control the high frequency modes ($> 1/\tau_0$) as τ_0^{m-1} , where τ_0 is a chosen frequency cut-off parameter. The low frequency modes ($\leq 1/\tau_0$) will be treated by the RCO technique for sufficiently small τ , which basically asserts that the error of the low frequency part behaves much better (satisfies the improved error bounds) as long as the time step size τ resolves the frequency. The regularity compensation oscillation (RCO) comes from the facts that the high modes are bounded by the regularity of the exact solution and an order of ε could be gained by noticing that $i\partial_t\psi + \Delta\psi = O(\varepsilon\psi)$ from (1.1), and respectively, an order of ε^2 could be gained by $i\partial_t\psi + \Delta\psi = O(\varepsilon^2|\psi|^2\psi)$ from (1.2), i.e., a suitable combination of higher order derivatives could compensate the wave oscillation of magnitude $O(\varepsilon)/O(\varepsilon^2)$.

The rest of this paper is organized as follows. In Section 2, the uniform error bound for the TSFP method in L^2 -norm for the Schrödinger equation with $O(\varepsilon)$ -potential up to the final time $T_\varepsilon = T/\varepsilon$ is proven and the error is shown to grow linearly with respect to T . Then, the improved uniform error bound in H^1 -norm is rigorously established with the help of a new technique of regularity compensation oscillation (RCO). In Section 3, the RCO technique is extended to analyze the improved uniform error bound in H^1 -norm for the cubic NLSE with $O(\varepsilon^2)$ -nonlinearity strength up to the final long-time at $O(1/\varepsilon^2)$. In Sections 2

& 3, extensive numerical results are reported to validate our error estimates and demonstrate that they are sharp. Finally, some conclusions are drawn in Section 4. Throughout the paper, the notation $A \lesssim B$ is used to represent that there exists a generic constant $C > 0$, which is independent of the mesh size h , time step τ and ε such that $|A| \leq CB$.

2 Improved uniform error bounds for the Schrödinger equation

In this section, we adopt the time-splitting Fourier pseudospectral (TSFP) method to numerically solve the Schrödinger equation (1.1) and rigorously establish the uniform error bound in L^2 -norm and improved uniform error bound in H^1 -norm using RCO. For the simplicity of presentation, we only carry out the analysis in one dimension (1D) and generalizations to higher dimensions are straightforward (see also Remark 2.5 for discussion). In 1D, the Schrödinger equation (1.1) with the initial data (1.3) and periodic boundary conditions on the domain $\Omega = (a, b)$ can be written as

$$\begin{cases} i\partial_t\psi(x, t) = -\Delta\psi(x, t) + \varepsilon V(x)\psi(x, t), & a < x < b, t > 0, \\ \psi(a, t) = \psi(b, t), \quad \partial_x\psi(a, t) = \partial_x\psi(b, t), & t \geq 0, \\ \psi(x, 0) = \psi_0(x), & x \in [a, b]. \end{cases} \quad (2.1)$$

2.1 The TSFP method

By the splitting technique [34, 35, 40], the Schrödinger equation (2.1) can be decomposed into two subproblems. The first one is

$$\begin{cases} i\partial_t\psi(x, t) = -\Delta\psi(x, t), & x \in \Omega, t > 0, \\ \psi(a, t) = \psi(b, t), \quad \partial_x\psi(a, t) = \partial_x\psi(b, t), & t \geq 0, \\ \psi(x, 0) = \psi_0(x), & x \in [a, b], \end{cases} \quad (2.2)$$

which can be solved exactly in phase space

$$\psi(\cdot, t) = e^{it\Delta}\psi_0(\cdot), \quad t \geq 0. \quad (2.3)$$

The second one is to solve

$$\begin{cases} i\partial_t\psi(x, t) = \varepsilon V(x)\psi(x, t), & x \in \Omega, t > 0, \\ \psi(x, 0) = \psi_0(x), & x \in [a, b], \end{cases} \quad (2.4)$$

which can be integrated exactly in time, for $x \in [a, b]$, as

$$\psi(x, t) = e^{-i\varepsilon t V(x)}\psi_0(x), \quad t \geq 0. \quad (2.5)$$

Choose $\tau > 0$ as the time step size and $t_n = n\tau$ for $n = 0, 1, \dots$ as the time steps. Denote $\psi^{[n]}(x)$ to be the approximation of $\psi(x, t_n)$ for $n \geq 0$, then a second-order semi-discretization of the Schrödinger equation (2.1) via the Strang splitting can be given as:

$$\psi^{[n+1]}(x) = \mathcal{S}_\tau(\psi^{[n]}) = e^{i\frac{\tau}{2}\Delta} e^{-i\varepsilon\tau V(x)} e^{i\frac{\tau}{2}\Delta} \psi^{[n]}(x), \quad x \in \overline{\Omega}, \quad (2.6)$$

with $\psi^{[0]}(x) = \psi_0(x)$.

In space, we discretize the Schrödinger equation (2.1) by the Fourier pseudospectral method. Let N be an even positive integer and choose the spatial mesh size $h = (b - a)/N$, then the grid points are given as

$$x_j := a + jh, \quad j \in \mathcal{T}_N^0 = \{j \mid j = 0, 1, \dots, N\}. \quad (2.7)$$

Denote $X_N := \{u = (u_0, u_1, \dots, u_N)^T \in \mathbb{C}^{N+1} \mid u_0 = u_N\}$ with the l^∞ -norm in X_N given as

$$\|u\|_{l^\infty} = \max_{0 \leq j \leq N-1} |u_j|, \quad u \in X_N. \quad (2.8)$$

Define $C_{\text{per}}(\Omega) = \{u \in C(\overline{\Omega}) \mid u(a) = u(b)\}$ and

$$Y_N := \text{span} \left\{ e^{i\mu_l(x-a)}, x \in \overline{\Omega}, l \in \mathcal{T}_N \right\}, \quad \mathcal{T}_N = \left\{ l \mid l = -\frac{N}{2}, \dots, \frac{N}{2} - 1 \right\},$$

where $\mu_l = \frac{2\pi l}{b-a}$. For any $u(x) \in C_{\text{per}}(\Omega)$ and a vector $u \in X_N$, let $P_N : L^2(\Omega) \rightarrow Y_N$ be the standard L^2 -projection operator onto Y_N , $I_N : C_{\text{per}}(\Omega) \rightarrow Y_N$ or $I_N : X_N \rightarrow Y_N$ be the trigonometric interpolation operator [36], i.e.,

$$P_N u = \sum_{l \in \mathcal{T}_N} \hat{u}_l e^{i\mu_l(x-a)}, \quad I_N u = \sum_{l \in \mathcal{T}_N} \tilde{u}_l e^{i\mu_l(x-a)}, \quad x \in \overline{\Omega},$$

where

$$\hat{u}_l = \frac{1}{b-a} \int_a^b u(x) e^{-i\mu_l(x-a)} dx, \quad \tilde{u}_l = \frac{1}{N} \sum_{j=0}^{N-1} u_j e^{-i\mu_l(x_j-a)}, \quad l \in \mathcal{T}_N,$$

with u_j interpreted as $u(x_j)$ when involved.

Let ψ_j^n be the numerical approximation of $\psi(x_j, t_n)$ for $j \in \mathcal{T}_N^0$ and $n \geq 0$, and denote $\psi^n = (\psi_0^n, \psi_1^n, \dots, \psi_N^n)^T \in X_N$ as the solution vector. Then, the time-splitting Fourier pseudospectral (TSFP) method for discretizing the Schrödinger equation (2.1) can be given for $n \geq 0$ as

$$\begin{aligned} \psi_j^{(1)} &= \sum_{l \in \mathcal{T}_N} e^{-i\frac{\tau\mu_l^2}{2}} \widetilde{(\psi^n)}_l e^{i\mu_l(x_j-a)}, \\ \psi_j^{(2)} &= e^{-i\varepsilon\tau V(x_j)} \psi_j^{(1)}, \quad j \in \mathcal{T}_N^0, \\ \psi_j^{n+1} &= \sum_{l \in \mathcal{T}_N} e^{-i\frac{\tau\mu_l^2}{2}} \widetilde{(\psi^{(2)})}_l e^{i\mu_l(x_j-a)}, \end{aligned} \quad (2.9)$$

where $\psi_j^0 = \psi_0(x_j)$ for $j \in \mathcal{T}_N^0$.

Remark 2.1 The second-order Strang splitting is used for discretizing the Schrödinger equation (2.1). It is straightforward to design the first-order scheme via the Lie splitting and higher order scheme via a higher order splitting method, e.g., the fourth-order compact splitting method or partitioned Runge-Kutta splitting method [7, 35, 41].

2.2 Local truncation error for the TSFP method

For proving the (improved) uniform error bounds, we give some results for the local truncation error in this subsection.

We assume the exact solution $\psi(x, t)$ of the Schrödinger equation (2.1) up to the time $T_\varepsilon = T/\varepsilon$ for any $T > 0$ satisfies

$$(A) \quad \|\psi(x, t)\|_{L^\infty([0, T_\varepsilon]; H_{\text{per}}^m)} \lesssim 1, \quad \|\partial_t \psi(x, t)\|_{L^\infty([0, T_\varepsilon]; H_{\text{per}}^{m-2})} \lesssim 1,$$

and the potential satisfies

$$(B) \quad V(x) \in H_{\text{per}}^{m^*}, \quad m^* = \max\{m, 5\},$$

where m describes the regularity of the exact solution. Here, $H_{\text{per}}^m(\Omega) = \{\phi \in H^m(\Omega) | \partial_x^k \phi(a) = \partial_x^k \phi(b), k = 0, 1, \dots, m-1\}$, with the equivalent H^m -norm on $H_{\text{per}}^m(\Omega)$ given as $\|\phi\|_{H^m} = \left(\sum_{l \in \mathbb{Z}} (1 + \mu_l^2)^m |\widehat{\phi}_l|^2 \right)^{1/2}$. In the rest of this paper, we may write $\psi(t) = \psi(x, t)$, i.e. omit the spatial variable, when there is no confusion. The following estimates of the local truncation error for the semi-discretization (2.6) hold.

Lemma 2.1 *Under assumptions (A) and (B) with $m \geq 3$, for $0 < \varepsilon \leq 1$, the local truncation error of the TSFP (2.9) for the Schrödinger equation with $O(\varepsilon)$ -potential at time t_n can be written as ($0 \leq n \leq T_\varepsilon/\tau - 1$)*

$$\mathcal{E}^n(x) := P_N \mathcal{S}_\tau(P_N \psi(t_n)) - P_N \psi(t_{n+1}) = P_N \mathcal{F}(P_N \psi(t_n)) + R_n, \quad (2.10)$$

where

$$\mathcal{F}(P_N \psi(t_n)) = -i\varepsilon\tau f^n\left(\frac{\tau}{2}\right) + i\varepsilon \int_0^\tau f^n(s) ds, \quad (2.11)$$

with $f^n(s) = e^{i(\tau-s)\Delta} V e^{is\Delta} P_N \psi(t_n)$, and the following error estimates hold

$$\|\mathcal{F}(P_N \psi(t_n))\|_{H^k} \lesssim \varepsilon\tau^3, \quad \|R_n\|_{H^k} \lesssim \varepsilon^2\tau^3 + \varepsilon\tau h^{m-k}, \quad k = 0, 1. \quad (2.12)$$

In addition, $\mathcal{E}^n(x), R_n(x) \in Y_N$ and the L^2 -estimates in (2.12) hold for $m \geq 2$.

Proof. The proof is standard following [34], and we sketch the procedure to emphasize the effects of spatial discretization and the parameter ε . By the Taylor expansion for $e^{-i\varepsilon\tau V}$, we have

$$\begin{aligned} P_N(\mathcal{S}_\tau(P_N \psi(t_n))) &= e^{i\tau\Delta} P_N \psi(t_n) - i\varepsilon\tau P_N \left(e^{i\frac{\tau}{2}\Delta} V e^{i\frac{\tau}{2}\Delta} P_N \psi(t_n) \right) \\ &\quad - \varepsilon^2\tau^2 P_N \left(\int_0^1 (1-\theta) e^{i\frac{\tau}{2}\Delta} e^{-i\varepsilon\theta\tau V} V^2 e^{i\frac{\tau}{2}\Delta} P_N \psi(t_n) d\theta \right). \end{aligned} \quad (2.13)$$

On the other hand, by repeatedly using the Duhamel's principle, we can write

$$\begin{aligned} P_N \psi(t_{n+1}) &= P_N \left(e^{i\tau\Delta} \psi(t_n) \right) - i\varepsilon P_N \left(\int_0^\tau e^{i(\tau-s)\Delta} V e^{is\Delta} \psi(t_n) ds \right) \\ &\quad - \varepsilon^2 P_N \left(\int_0^\tau \int_0^s e^{i(\tau-s)\Delta} V e^{i(s-w)\Delta} V \psi(t_n + w) dw ds \right). \end{aligned}$$

Recalling assumptions (A) and (B), applying Fourier projections, we have

$$\begin{aligned} P_N \psi(t_{n+1}) &= e^{i\tau\Delta} P_N \psi(t_n) - i\varepsilon \int_0^\tau P_N \left(e^{i(\tau-s)\Delta} V e^{is\Delta} P_N \psi(t_n) \right) ds \\ &\quad - \varepsilon^2 \int_0^\tau \int_0^s P_N \left(e^{i(\tau-s)\Delta} V e^{i(s-w)\Delta} V P_N \psi(t_n + w) \right) dw ds - r_h^n, \end{aligned} \quad (2.14)$$

with $\|r_h^n(x)\|_{L^2} \lesssim \varepsilon\tau h^m$ and $\|r_h^n(x)\|_{H^1} \lesssim \varepsilon\tau h^{m-1}$. Introducing $f^n(s)$ as in Lemma 2.1 and

$$B^n(s, w) = P_N \left(e^{i(\tau-s)\Delta} V e^{i(s-w)\Delta} V e^{iw\Delta} P_N \psi(t_n) \right),$$

the local truncation error can be written as [34]

$$\mathcal{E}^n = P_N \mathcal{F}(P_N \psi(t_n)) - \frac{\varepsilon^2 \tau^2}{2} B^n \left(\frac{\tau}{2}, \frac{\tau}{2} \right) + \varepsilon^2 \int_0^\tau \int_0^s B^n(s, w) dw ds + \varepsilon^2 r_1^n + \varepsilon^2 r_2^n + r_h^n,$$

where $\mathcal{F}(P_N \psi(t_n))$ is given in (2.11) and

$$\begin{aligned} r_1^n &= -\tau^2 \int_0^1 (1-\theta) P_N \left(e^{i\frac{\tau}{2}\Delta} (e^{-i\varepsilon\theta\tau V} - 1) V^2 e^{i\frac{\tau}{2}\Delta} P_N \psi(t_n) \right) d\theta, \\ r_2^n &= \int_0^\tau \int_0^s \left(P_N \left(e^{i(\tau-s)\Delta} V e^{i(s-w)\Delta} V P_N \psi(t_n + w) \right) - B^n(s, w) \right) dw ds. \end{aligned}$$

Since $e^{i\tau\Delta}$ preserves the H^s -norm and $\|(e^{-i\varepsilon\theta\tau V} - 1)V^2\|_{H^1} \lesssim \varepsilon\tau\theta\|V\|_{H^1}^3$, we have

$$\|r_1^n\|_{H^1} \lesssim \varepsilon\tau^3 \|V\|_{H^1}^3 \|\psi(t_n)\|_{H^1} \lesssim \varepsilon\tau^3.$$

The following estimates are standard (c.f. [34]),

$$\begin{aligned} \|r_2^n\|_{H^1} &\lesssim \tau^3 \|V\|_{H^1}^2 \|\partial_s \psi(\cdot)\|_{L^\infty([0, \tau]; H^1)} \lesssim \tau^3, \\ \left\| -\frac{\tau^2}{2} B \left(\frac{\tau}{2}, \frac{\tau}{2} \right) + \int_0^\tau \int_0^s B(s, w) dw ds \right\|_{H^1} &\lesssim \tau^3 \|V\|_{H^3}^2 \|\psi(t_n)\|_{H^3} \lesssim \tau^3. \end{aligned}$$

Finally, for the major part of the local truncation error can be estimated by the midpoint quadrature rule as [34]

$$\|\mathcal{F}(P_N \psi(t_n))\|_{H^1} \lesssim \varepsilon\tau^3 \|[\Delta, [\Delta, V]] P_N \psi(t_n)\|_{H^1} \lesssim \|V\|_{H^5} \|\psi(t_n)\|_{H^3}, \quad (2.15)$$

where $[\Delta, [\Delta, V]]$ is the double commutator. Thus, by setting

$$R_n = -\frac{\varepsilon^2 \tau^2}{2} B^n \left(\frac{\tau}{2}, \frac{\tau}{2} \right) + \varepsilon^2 \int_0^\tau \int_0^s B^n(s, w) dw ds + \varepsilon^2 r_1^n + \varepsilon^2 r_2^n + r_h^n, \quad (2.16)$$

we obtain the estimates in Lemma 2.1. \square

2.3 Uniform error bounds in L^2 -norm

In this subsection, we adopt the unitarity of the numerical solution flow in $L^2(\Omega)$ to establish the uniform error bound in L^2 -norm with linear growth in T up to the time $T_\varepsilon = \frac{T}{\varepsilon}$. We remark that the uniform estimates are standard, while the linear growth of the error only holds in the L^2 -norm. The reason is that TSFP (2.9) only preserves the L^2 -norm.

Theorem 2.1 *Let ψ^n be the numerical approximation obtained from the TSFP (2.9). Under assumptions (A) and (B) with $m \geq 2$, for any $0 < \varepsilon \leq 1$, we have*

$$\|\psi(x, t_n) - I_N \psi^n\|_{L^2} \leq (C_0 + C_1 T) \left(h^m + \tau^2 \right), \quad 0 \leq n \leq \frac{T/\varepsilon}{\tau}, \quad (2.17)$$

where C_0 and C_1 are two positive constants independent of h , τ , n , ε and T .

Proof. Noticing that

$$I_N \psi^n - \psi(t_n) = I_N \psi^n - P_N(\psi(t_n)) + P_N(\psi(t_n)) - \psi(t_n), \quad (2.18)$$

under assumptions (A) and (B), we get from the standard Fourier projection properties [36]

$$\|I_N \psi^n - \psi(t_n)\|_{L^2} \leq \|I_N \psi^n - P_N(\psi(t_n))\|_{L^2} + C_2 h^m, \quad 0 \leq n \leq \frac{T/\varepsilon}{\tau}. \quad (2.19)$$

Thus, it suffice to consider the error function $e^n \in Y_N$ at t_n as

$$e^n := e^n(x) = I_N \psi^n - P_N \psi(t_n), \quad 0 \leq n \leq \frac{T/\varepsilon}{\tau}, \quad (2.20)$$

and $\|e^0\|_{L^2} \leq C_3 h^m$ implied by the standard projection and interpolation results. From the local error (2.10) in Lemma 2.1, we have the error equation for e^n ($0 \leq n \leq \frac{T/\varepsilon}{\tau} - 1$),

$$e^{n+1} = I_N \psi^{n+1} - P_N \psi(t_{n+1}) = I_N \psi^{n+1} - P_N \mathcal{S}_\tau(P_N \psi(t_n)) + \mathcal{E}^n. \quad (2.21)$$

Noticing the fully discrete scheme (2.9) and \mathcal{S}_τ (2.6), i.e.

$$\begin{aligned} I_N \psi^{n+1} &= e^{i\frac{\tau}{2}\Delta} (I_N \psi^{(2)}), \quad I_N(\psi^{(2)}) = I_N(e^{-i\varepsilon\tau V(x)} \psi^{(1)}), \quad I_N \psi^{(1)} = e^{i\frac{\tau}{2}\Delta} I_N \psi^n, \\ P_N(\mathcal{S}_\tau(\psi(t_n))) &= e^{i\frac{\tau}{2}\Delta} (P_N \psi^{(2)}), \quad \psi^{(2)} = e^{-i\varepsilon\tau V(x)} \psi^{(1)}, \quad \psi^{(1)} = e^{i\frac{\tau}{2}\Delta} P_N \psi(t_n), \end{aligned}$$

in view of the facts that I_N and P_N are identical on Y_N and $e^{i\tau\Delta/2}$ preserves the H^k -norm ($k \geq 0$), using Taylor expansion $e^{-i\varepsilon\tau V(x)} = 1 - i\varepsilon\tau V(x) \int_0^1 e^{-i\varepsilon\theta\tau V(x)} d\theta$ and assumptions (A) and (B), we have

$$\|I_N \psi^{n+1} - P_N \mathcal{S}_\tau(P_N \psi(t_n))\|_{L^2} = \|I_N \psi^{(2)} - P_N \psi^{(2)}\|_{L^2}, \quad (2.22)$$

$$\begin{aligned} \|P_N \psi^{(2)} - I_N \psi^{(2)}\|_{L^2} &= \left\| \varepsilon\tau (P_N - I_N) \left(V(x) \int_0^1 e^{-i\varepsilon\theta\tau V(x)} d\theta \psi^{(1)} \right) \right\|_{L^2} \\ &\leq C_4 \varepsilon\tau h^m, \end{aligned} \quad (2.23)$$

where C_4 is obtained from Fourier interpolation and projection properties together with $\left\| \left(V(x) \int_0^1 e^{-i\varepsilon\theta\tau V(x)} d\theta \psi^{(1)} \right) \right\|_{H^m} \leq C(\|V\|_{H^m}) \|\psi(t_n)\|_{H^m}$. In addition, by direct computation and Parseval's identity, we can derive

$$\begin{aligned} \|I_N \psi^{(2)} - I_N \psi^{(2)}\|_{L^2} &= \sqrt{h \sum_{j=0}^{N-1} |\psi_j^{(2)} - \psi^{(2)}(x_j)|^2} = \sqrt{h \sum_{j=0}^{N-1} |\psi_j^{(1)} - \psi^{(1)}(x_j)|^2} \\ &= \|I_N \psi^{(1)} - I_N \psi^{(1)}\|_{L^2} = \|I_N \psi^n - P_N \psi(t_n)\|_{L^2} \\ &= \|e^n\|_{L^2}. \end{aligned} \quad (2.24)$$

Taking the L^2 -norm on both sides of (2.21) and combining (2.22), (2.23) and (2.24) together, in view of Lemma 2.1, we obtain for $0 \leq n \leq \frac{T/\varepsilon}{\tau} - 1$,

$$\begin{aligned} \|e^{n+1}\|_{L^2} &\leq \|\mathcal{E}^n\|_{L^2} + \|I_N \psi^{(2)} - P_N \psi^{(2)}\|_{L^2} \\ &\leq \|\mathcal{E}^n\|_{L^2} + \|I_N \psi^{(2)} - I_N \psi^{(2)}\|_{L^2} + \|P_N \psi^{(2)} - I_N \psi^{(2)}\|_{L^2} \\ &\leq \|e^n\|_{L^2} + C_5 (\varepsilon \tau h^m + \varepsilon \tau^3). \end{aligned} \quad (2.25)$$

Thus, the following estimates hold

$$\|e^{n+1}\|_{L^2} \leq C_5 T (h^m + \tau^2) + C_3 h^m, \quad 0 \leq n \leq \frac{T/\varepsilon}{\tau} - 1, \quad (2.26)$$

and the conclusion of Theorem 2.1 by taking $C_0 = C_2 + C_3$ and $C_1 = C_5$ in view of (2.19). It is easy to verify all the constants appearing in the proof only depend on V and ψ . \square

Remark 2.2 According to Theorem 2.1, the uniform error bound for the TSFP method in L^2 -norm for the Schrödinger equation linearly grows with respect to T , and the results can be generalized to other splitting methods. In fact, given an accuracy bound $\delta_0 > 0$, the time for the second-order splitting method to violate the accuracy requirement δ_0 is $O(\delta_0/\tau^2)$. For the first-order and fourth-order splitting methods, the time is $O(\delta_0/\tau)$ and $O(\delta_0/\tau^4)$, respectively. In other words, higher order splitting method performs much better in the long-time simulations not only regarding the higher accuracy but also longer simulation time to produce accurate solutions. For the L^2 -estimates in Theorem 2.1, the regularity requirements on the potential $V(x)$ can be weakened. In addition, extensions to 2D/3D are straightforward.

Remark 2.3 By the similar procedure (or formally letting $h \rightarrow 0^+$), we could establish uniform error bounds for the semi-discretization. Let $\psi^{[n]}$ be the numerical approximation obtained from the Strang splitting (2.6). Under assumptions (A) and (B) with $m \geq 3$, for any $0 < \varepsilon \leq 1$, we have

$$\|\psi(x, t_n) - \psi^{[n]}\|_{L^2} \leq C_0 T \tau^2, \quad 0 \leq n \leq \frac{T/\varepsilon}{\tau}, \quad (2.27)$$

where C_0 is a positive constant independent of τ , n , ε and T .

2.4 Improved uniform error bounds in H^1 -norm

In this subsection, we show improved uniform error bounds in H^1 -norm for the Schrödinger equation with $O(\varepsilon)$ -potential up to the time $T_\varepsilon = T/\varepsilon$ under assumptions (A) and (B) with $m \geq 3$, where we will work with H^1 -estimates for the nonlinear case also to control the nonlinearity in 1D. It is worth noticing that in higher dimensions (2D/3D), H^2 -estimates would be enough.

Theorem 2.2 *Let ψ^n be the numerical approximation obtained from the TSFP (2.9). Under the assumptions (A) and (B) with $m \geq 3$, for $h_0 > 0$ and $0 < \tau_0 < 1$ sufficiently small and independent of ε such that, for any $0 < \varepsilon \leq 1$, when $0 < h \leq h_0$ and $0 < \tau < \alpha \frac{(b-a)^2}{2(1+\tau_0)^2\pi} \tau_0^2$ for a fixed constant $\alpha \in (0, 1)$, we have*

$$\|\psi(x, t_n) - I_N \psi^n\|_{H^1} \lesssim h^{m-1} + \varepsilon \tau^2 + \tau_0^{m-1}, \quad 0 \leq n \leq \frac{T/\varepsilon}{\tau}. \quad (2.28)$$

In particular, if the exact solution is sufficiently smooth, e.g. $\psi(x, t) \in H_{\text{per}}^\infty$, the τ_0^{m-1} part error would become extremely small for small enough τ_0 and can be ignored practically, where the improved error bounds for sufficiently small τ could be stated as

$$\|\psi(x, t_n) - I_N \psi^n\|_{H^1} \lesssim h^{m-1} + \varepsilon \tau^2, \quad 0 \leq n \leq \frac{T/\varepsilon}{\tau}. \quad (2.29)$$

Remark 2.4 Before the presentation of the proof, some observations are marked. First, $1/\tau_0 > 1$ serves as a cut-off mode, i.e. the modes $|l| > 1/\tau_0$ are treated by Fourier projection, and the modes $|l| \leq \frac{1}{\tau_0}$ will be treated by the RCO technique for $\tau < \frac{(b-a)^2}{2\pi} \tau_0^2$. The requirement on τ is that the step size has to resolve the largest oscillatory frequency of the free Schrödinger operator below the cut-off modes as $|\mu_l|^2 = \frac{4l^2\pi^2}{(b-a)^2} \sim \frac{4\pi^2}{(b-a)^2\tau_0^2}$, i.e. $\tau|\mu_l|^2 < 2\pi$.

Proof. Following the proof of Theorem 2.1, we only need estimate the error e^n in (2.20) for $0 \leq n \leq \frac{T/\varepsilon}{\tau}$. Firstly, using the fact that $P_N = I_N$ when restricted on Y_N , we can write for $0 \leq n \leq \frac{T/\varepsilon}{\tau}$,

$$I_N \psi^{n+1} - P_N \mathcal{S}_\tau(P_N \psi(t_n)) = e^{i\tau\Delta} (I_N \psi^n - P_N \psi(t_n)) + Q^n(x), \quad (2.30)$$

where $Q^n(x) \in Y_N$ is given by

$$\begin{aligned} Q^n(x) &= -i\varepsilon\tau e^{i\frac{\tau}{2}\Delta} \left(I_N \left(V(x) \int_0^1 e^{-i\varepsilon\theta\tau V(x)} d\theta \psi^{(1)} \right) \right) \\ &\quad + i\varepsilon\tau e^{i\frac{\tau}{2}\Delta} \left(P_N \left(V(x) \int_0^1 e^{-i\varepsilon\theta\tau V(x)} d\theta \psi^{(1)} \right) \right). \end{aligned} \quad (2.31)$$

Using Parseval's identity and finite difference operator (c.f. [3,4]), by the similar estimates (2.22), (2.23) and (2.24) for the L^2 -norm case, we can control Q^n as

$$\|Q^n\|_{H^1} \lesssim \varepsilon\tau \left(h^{m-1} + \|e^n\|_{H^1} \right), \quad 0 \leq n \leq \frac{T/\varepsilon}{\tau} - 1. \quad (2.32)$$

From (2.30) and (2.21), we could derive that for $0 \leq n \leq \frac{T/\varepsilon}{\tau} - 1$,

$$e^{n+1} = e^{i\tau\Delta} e^n + Q^n(x) + \mathcal{E}^n, \quad (2.33)$$

which implies

$$e^{n+1} = e^{i(n+1)\tau\Delta} e^0 + \sum_{k=0}^n e^{i(n-k)\tau\Delta} \left(Q^k(x) + \mathcal{E}^k \right). \quad (2.34)$$

Step 1. (Identifying the leading error term) Using the local truncation error representation (2.12) in Lemma 2.1, we have

$$\sum_{k=0}^n e^{i(n-k)\tau\Delta} \mathcal{E}^k = \sum_{k=0}^n e^{i(n-k)\tau\Delta} (P_N \mathcal{F}(P_N \psi(t_k)) + R_k), \quad (2.35)$$

and

$$\left\| \sum_{k=0}^n e^{i(n-k)\tau\Delta} R_k \right\|_{H^1} \lesssim (n+1) \left(\varepsilon^2 \tau^3 + \varepsilon \tau h^{m-1} \right) \lesssim T \varepsilon \tau^2 + T h^{m-1}, \quad (2.36)$$

$$\left\| \sum_{k=0}^n e^{i(n-k)\tau\Delta} Q^k(x) \right\|_{H^1} \lesssim \varepsilon \tau \sum_{k=0}^n \|e^k\|_{H^1} + h^{m-1}. \quad (2.37)$$

Combining above estimates and $\|e^0\|_{H^1} \lesssim h^{m-1}$, we obtain for $0 \leq n \leq \frac{T/\varepsilon}{\tau} - 1$,

$$\begin{aligned} \|e^{n+1}\|_{H^1} &\lesssim h^{m-1} + \varepsilon \tau^2 + \varepsilon \tau \sum_{k=0}^n \|e^k\|_{H^1} \\ &\quad + \left\| \sum_{k=0}^n e^{i(n-k)\tau\Delta} P_N \mathcal{F}(P_N \psi(t_k)) \right\|_{H^1}. \end{aligned} \quad (2.38)$$

Recalling Lemma 2.1, we have $\|\mathcal{F}(P_N \psi(t_k))\|_{H^1} \lesssim \tau^3$, which implies $\|e^{n+1}\|_{H^1} \lesssim \tau^2 + h^{m-1}$. Thus, to prove the improved error estimates, we need analyze the last term in (2.38) carefully, i.e., treat the sum $\sum_{k=0}^n e^{i(n-k)\tau\Delta} P_N \mathcal{F}(P_N \psi(t_k))$ in a proper way. To gain an order of $O(\varepsilon)$ from the sum, we shall introduce the **regularity compensated oscillation** (RCO) technique. From (1.1), we find $\partial_t \psi(x, t) - i\Delta \psi(x, t) = O(\varepsilon)$, and it is natural to introduce the ‘twisted variable’ as

$$\phi(x, t) = e^{-it\Delta} \psi(x, t), \quad t \geq 0, \quad (2.39)$$

and $\phi(t) := \phi(x, t)$ satisfies the equation

$$i\partial_t \phi(x, t) = \varepsilon e^{-it\Delta} \left(V(x) e^{it\Delta} \phi(x, t) \right), \quad t > 0. \quad (2.40)$$

It is direct to see that $\phi(x, t)$ enjoys the same H^k ($k \geq 0$) bounds as $\psi(x, t)$, while

$$\|\partial_t \phi(t)\|_{H^m} \lesssim \varepsilon, \quad 0 \leq t \leq T/\varepsilon. \quad (2.41)$$

The RCO approach would then perform a summation by parts procedure in $\sum_{k=0}^n e^{i(n-k)\tau\Delta} P_N \mathcal{F}(P_N \psi(t_k))$ to force $\partial_t \phi(t)$ appear with a gain of order $O(\varepsilon)$, where τ is small to control the accumulation of the phase (frequency) of the type $e^{i(n-k)\tau\Delta}$. Since the number N of the spatial grid points could be very large, we shall introduce a cut-off parameter $\tau_0 \in (0, 1)$, where the high frequency modes ($|l| > \frac{1}{\tau_0}$) will be controlled by the smoothness of the exact solution and the Fourier

projections, and the low frequency modes ($|l| \leq \frac{1}{\tau_0}$) will be dealt with the RCO technique.

Cut-off parameter. Choose $\tau_0 \in (0, 1)$, and let $N_0 = 2\lceil 1/\tau_0 \rceil \in \mathbb{Z}^+$ ($\lceil \cdot \rceil$ is the ceiling function) with $1/\tau_0 \leq N_0/2 < 1 + 1/\tau_0$, then only those Fourier modes with $-\frac{N_0}{2} \leq l \leq \frac{N_0}{2} - 1$ in $\mathcal{F}(P_N\psi(t_k))$ would be considered. Based on the Fourier projections and the assumption (A), we have $\|P_{N_0}\psi(x, t) - P_N\psi(x, t)\|_{L^\infty([0, T/\varepsilon]; H^1)} \lesssim h^{m-1} + N_0^{1-m} \lesssim h^{m-1} + \tau_0^{m-1}$ and for $0 \leq n \leq \frac{T/\varepsilon}{\tau} - 1$,

$$\|P_{N_0}\mathcal{F}(P_{N_0}\psi(t_n)) - P_N\mathcal{F}(P_N\psi(t_n))\|_{H^1} \lesssim \varepsilon\tau(h^{m-1} + \tau_0^{m-1}). \quad (2.42)$$

Indeed, since $P_N\psi(t_k) \in Y_N$, we could actually assume the choice of τ_0 such that $N_0 \leq N$, but here we work without this condition for the convenience of extension to the semi-discretization-in-time case.

Based on (2.38), (2.39) and (2.42), recalling the unitary properties of $e^{it\Delta}$, we find for $0 \leq n \leq \frac{T/\varepsilon}{\tau} - 1$,

$$\|e^{n+1}\|_{H^1} \lesssim h^{m-1} + \tau_0^{m-1} + \varepsilon\tau^2 + \varepsilon\tau \sum_{k=0}^n \|e^k\|_{H^1} + \|\mathcal{R}^n\|_{H^1}, \quad (2.43)$$

$$\mathcal{R}^n(x) = \sum_{k=0}^n e^{-i(k+1)\tau\Delta} P_{N_0}\mathcal{F}(e^{it_k\Delta}(P_{N_0}\phi(t_k))). \quad (2.44)$$

Step 2. (Analysis via RCO) Let $\phi(t) = \sum_{l \in \mathbb{Z}} \widehat{\phi}_l(t) e^{i\mu_l(x-a)}$ ($t \geq 0$), and we have $P_{N_0}\phi(t) = \sum_{l \in \mathcal{T}_{N_0}} \widehat{\phi}_l(t) e^{i\mu_l(x-a)}$, where $\widehat{\phi}_l(t)$ is the l -th Fourier coefficient of $\phi(x, t)$. For $l \in \mathcal{T}_{N_0}$, introduce the multi-index set $\mathcal{I}_l^{N_0}$ associated with l as

$$\mathcal{I}_l^{N_0} = \{(l_1, l_2) \mid l_1 + l_2 = l, l_1 \in \mathbb{Z}, l_2 \in \mathcal{T}_{N_0}\}. \quad (2.45)$$

According to the definition of \mathcal{F} in Lemma 2.1, we have the expansion

$$e^{-i(k+1)\tau\Delta} P_{N_0} \left(e^{i(\tau-s)\Delta} V e^{is\Delta} P_{N_0}\psi(t_n) \right) = \sum_{l \in \mathcal{T}_{N_0}} \sum_{(l_1, l_2) \in \mathcal{I}_l^{N_0}} \mathcal{G}_{k, l, l_1, l_2}(s) e^{i\mu_l(x-a)},$$

where $\mathcal{G}_{k, l, l_1, l_2}(s)$ ($l, l_2 \in \mathcal{T}_{N_0}$) is a function of s as

$$\mathcal{G}_{k, l, l_1, l_2}(s) = e^{i(t_k+s)\delta_{l, l_2}} \widehat{V}_{l_1} \widehat{\phi}_{l_2}(t_k), \quad \delta_{l, l_2} = \delta_l - \delta_{l_2}, \quad \delta_l = \mu_l^2. \quad (2.46)$$

Then, the remainder term $\mathcal{R}^n(x)$ in (2.43) reads

$$\mathcal{R}^n(x) = i\varepsilon \sum_{k=0}^n \sum_{l \in \mathcal{T}_{N_0}} \sum_{(l_1, l_2) \in \mathcal{I}_l^{N_0}} \lambda_{k, l, l_1, l_2} e^{i\mu_l(x-a)}, \quad (2.47)$$

where the coefficients λ_{k, l, l_1, l_2} are given by

$$\lambda_{k, l, l_1, l_2} = -\tau \mathcal{G}_{k, l, l_1, l_2}(\tau/2) + \int_0^\tau \mathcal{G}_{k, l, l_1, l_2}(s) ds = r_{l, l_2} e^{it_k \delta_{l, l_2}} c_{k, l, l_1, l_2}, \quad (2.48)$$

and

$$c_{k, l, l_1, l_2} = \widehat{V}_{l_1} \widehat{\phi}_{l_2}(t_k), \quad r_{l, l_2} = -\tau e^{i\frac{\tau \delta_{l, l_2}}{2}} + \int_0^\tau e^{is\delta_{l, l_2}} ds = O(\tau^3 (\delta_{l, l_2})^2). \quad (2.49)$$

The key observation from (2.49) is: if $\delta_{l,l_2} = 0$, $r_{l,l_2} = 0$ and the term λ_{k,l,l_1,l_2} in (2.48) vanishes. Thus, in the discussion below, we shall assume that $\delta_{l,l_2} \neq 0$. Based on the RCO, we will go through the detailed structure of (2.47) and exchange the order of summation (sum over index k first), which will result in the terms like $\phi(t_k) - \phi(t_{k+1}) = O(\tau \partial_t \phi) = O(\varepsilon \tau)$ to gain an order of ε .

First, for $l \in \mathcal{T}_{N_0}$ and $(l_1, l_2) \in \mathcal{I}_l^{N_0}$, we have

$$|\delta_{l,l_2}| \leq \delta_{N_0/2} = \mu_{N_0/2}^2 = (\pi N_0)^2 / (b-a)^2 \leq \frac{4\pi^2(1+\tau_0)^2}{\tau_0^2(b-a)^2}, \quad (2.50)$$

which implies the following estimates for $0 < \tau \leq \alpha \frac{(b-a)^2}{2(1+\tau_0)^2\pi} \tau_0^2$ with $\alpha \in (0, 1)$ and $\tau_0 \in (0, 1)$

$$\frac{\tau}{2} |\delta_{l,l_2}| < \alpha\pi. \quad (2.51)$$

Denoting $S_{n,l,l_2} = \sum_{k=0}^n e^{it_k \delta_{l,l_2}}$ ($n \geq 0$) and using summation by parts, we find from (2.48) that

$$\sum_{k=0}^n \lambda_{k,l,l_1,l_2} = r_{l,l_2} \sum_{k=0}^{n-1} S_{k,l,l_2} (c_{k,l,l_1,l_2} - c_{k+1,l,l_1,l_2}) + S_{n,l,l_2} r_{l,l_2} c_{n,l,l_1,l_2}, \quad (2.52)$$

and

$$c_{k,l,l_1,l_2} - c_{k+1,l,l_1,l_2} = \widehat{V}_{l_1} \left(\widehat{\phi}_{l_2}(t_k) - \widehat{\phi}_{l_2}(t_{k+1}) \right). \quad (2.53)$$

For $0 < \tau \leq \alpha \frac{(b-a)^2}{2(1+\tau_0)^2\pi} \tau_0^2$, we know from (2.51) that

$$|S_{n,l,l_2}| \leq \frac{2}{|1 - e^{i\tau \delta_{l,l_2}}|} = \frac{1}{|\sin(\tau \delta_{l,l_2}/2)|} \leq \frac{C}{\tau |\delta_{l,l_2}|}, \quad \forall n \geq 0, \quad (2.54)$$

where we have used the fact $\frac{\sin(s)}{s}$ is bounded (decreasing) for $s \in [0, \alpha\pi)$ and $C = \frac{2\alpha\pi}{\sin(\alpha\pi)}$ (noticing the case $\delta_{l,l_2} = 0$ is trivial and δ_{l,l_2} is assumed to be nonzero here). Combining (2.49), (2.52), (2.53) and (2.54), we have

$$\left| \sum_{k=0}^n \lambda_{k,l,l_1,l_2} \right| \lesssim \tau^2 |\delta_{l,l_2}| |\widehat{V}_{l_1}| \left[\sum_{k=0}^{n-1} \left| \widehat{\phi}_{l_2}(t_k) - \widehat{\phi}_{l_2}(t_{k+1}) \right| + \left| \widehat{\phi}_{l_2}(t_n) \right| \right]. \quad (2.55)$$

We note that (2.55) is the key for the refined estimate, where we shall gain an order of ε from the $\phi(t_k) - \phi(t_{k+1})$ terms (see (2.41)). Of course, the condition (2.51) is also important to exclude the resonant case where S_n could be unbounded, i.e., (2.51) makes the estimate (2.55) available.

Step 3. (Improved estimates) Now, we are ready to give the improved estimates. For $l \in \mathcal{T}_{N_0}$ and $(l_1, l_2) \in \mathcal{I}_l^{N_0}$, simple calculations show ($l = l_1 + l_2$)

$$1 + \mu_l^2 \leq (1 + \mu_{l_1}^2)(1 + \mu_{l_2}^2), \quad |\delta_{l,l_2}| \leq (1 + \mu_{l_1}^2)(1 + \mu_{l_2}^2). \quad (2.56)$$

Based on (2.47), (2.55) and (2.56), using Cauchy inequality, we now estimate the remainder term in (2.43),

$$\begin{aligned}
& \|\mathcal{R}^n(x)\|_{H^1}^2 \tag{2.57} \\
&= \varepsilon^2 \sum_{l \in \mathcal{T}_{N_0}} (1 + \mu_l^2) \left| \sum_{(l_1, l_2) \in \mathcal{I}_l^{N_0}} \sum_{k=0}^n \lambda_{k, l_1, l_2} \right|^2 \\
&\lesssim \varepsilon^2 \tau^4 \left\{ \sum_{l \in \mathcal{T}_{N_0}} \left(\sum_{(l_1, l_2) \in \mathcal{I}_l^{N_0}} |\widehat{V}_{l_1}| \left| \widehat{\phi}_{l_2}(t_n) \right| \prod_{j=1}^2 (1 + \mu_{l_j}^2)^{3/2} \right)^2 \right. \\
&\quad \left. + n \sum_{k=0}^{n-1} \left[\sum_{l \in \mathcal{T}_{N_0}} \left(\sum_{(l_1, l_2) \in \mathcal{I}_l^{N_0}} |\widehat{V}_{l_1}| \left| \widehat{\phi}_{l_2}(t_k) - \widehat{\phi}_{l_2}(t_{k+1}) \right| \prod_{j=1}^2 (1 + \mu_{l_j}^2)^{3/2} \right)^2 \right] \right\}.
\end{aligned}$$

To estimate each term in (2.57), we use the auxiliary function $\xi(x) = \sum_{l \in \mathbb{Z}} (1 + \mu_l^2)^{3/2} |\widehat{\phi}_l(t_n)| e^{i\mu_l(x-a)}$, where $\xi(x) \in H_{\text{per}}^{m-3}(\Omega)$ implied by the assumption (A) and $\|\xi(x)\|_{H^s} \lesssim \|\phi(t_n)\|_{H^{s+3}}$ ($s \leq m-3$). Similarly, introduce the function $U(x) = \sum_{l \in \mathbb{Z}} (1 + \mu_l^2)^{3/2} |\widehat{V}_l| e^{i\mu_l(x-a)}$, where $U(x) \in H_{\text{per}}^2$ implied by the assumption (B). Expanding

$$U(x)\xi(x) = \sum_{l \in \mathbb{Z}} \sum_{l_1+l_2=l} \prod_{j=1}^2 (1 + \mu_{l_j}^2)^{3/2} |\widehat{V}_{l_1}| |\widehat{\phi}_{l_2}(t_n)| e^{i\mu_l(x-a)},$$

we could obtain

$$\begin{aligned}
& \sum_{l \in \mathcal{T}_{N_0}} \left(\sum_{(l_1, l_2) \in \mathcal{I}_l^{N_0}} |\widehat{V}_{l_1}| |\widehat{\phi}_{l_2}(t_n)| \prod_{j=1}^2 (1 + \mu_{l_j}^2)^{3/2} \right)^2 \\
&\leq \|U(x)\xi(x)\|_{L^2}^2 \lesssim \|V(x)\|_{H^4}^2 \|\phi(t_k)\|_{H^3}^2 \lesssim 1, \tag{2.58}
\end{aligned}$$

which together with (2.41) implies (applying the same trick to the rest terms) for $0 \leq n \leq \frac{T/\varepsilon}{\tau} - 1$,

$$\begin{aligned}
\|\mathcal{R}^n(x)\|_{H^1}^2 &\lesssim \varepsilon^2 \tau^4 \left(\|\phi(t_k)\|_{H^3}^2 + n \sum_{k=0}^{n-1} \|\phi(t_k) - \phi(t_{k+1})\|_{H^3}^2 \right) \\
&\lesssim \varepsilon^2 \tau^4 + n^2 \varepsilon^4 \tau^6 \|\partial_t \phi(x, t)\|_{L^\infty([0, T_\varepsilon]; H^3)}^2 \lesssim \varepsilon^2 \tau^4. \tag{2.59}
\end{aligned}$$

Combining (2.43) and (2.59), we have

$$\|e^{n+1}\|_{H^1} \lesssim h^{m-1} + \tau_0^{m-1} + \varepsilon \tau^2 + \varepsilon \tau \sum_{k=0}^n \|e^k\|_{H^1}, \quad 0 \leq n \leq \frac{T/\varepsilon}{\tau} - 1. \tag{2.60}$$

Discrete Gronwall's inequality would yield $\|e^{n+1}\|_{H^1} \lesssim h^{m-1} + \varepsilon \tau^2 + \tau_0^{m-1}$ ($0 \leq n \leq \frac{T/\varepsilon}{\tau} - 1$), and the proof for the improved uniform error bound (2.17) in Theorem 2.2 is completed. \square

Remark 2.5 From the proof, the key steps of RCO are the cut-off (2.42) to separate the high/low Fourier modes, sufficiently small time step size τ to compensate the growth of errors at low Fourier modes via expansion (cf. (2.51),(2.54) and (2.55)), and the estimates of the Fourier coefficients (cf. (2.59)). Here, the special structure of the Fourier functions are important, e.g. $e^{i\mu_l(x-a)}e^{i\mu_k(x-a)} = e^{i\mu_{l+k}(x-a)}$. Based on above observations, it is straightforward to extend the RCO analysis to the higher dimensions (2D/3D) in rectangular domain with periodic boundary conditions, as the higher dimensional tensor Fourier basis enjoy the same properties ensuring the Fourier expansion for products of periodic functions.

Remark 2.6 In the proof, (2.51),(2.54) and (2.55) suggest the two order spatial regularity is regained from the summation by parts process indicated by $1/(\tau\delta_{l,l_2})$ (δ_{l,l_2} is roughly Δ). Usually, such gained regularity will be lost when considering the other term of the summation by parts, i.e. the terms corresponding to $\phi(t_k) - \phi(t_{k+1}) = O(\tau\partial_t\phi)$, where ∂_t term will compensate the regularity gain from δ_{l,l_2} . However, as we have chosen a particularly designed twisted variable $\phi(t)$, there will be no regularity loss in $\phi(t_k) - \phi(t_{k+1})$, but with a gain of order ε .

2.5 Numerical results

In this subsection, we present numerical results of the TSFP method for the long-time dynamics of the Schrödinger equation with $O(\varepsilon)$ -potential in 1D, up to the time $T_\varepsilon = \frac{T}{\varepsilon}$.

First, we show an example to confirm that the uniform error bound in L^2 -norm linearly grows with respect to T . We choose the potential $V(x) = 5\cos(2\pi x)$ and the H_{per}^2 initial data as

$$\psi_0(x) = 5x^2(1-x)^2, \quad x \in [0, 1]. \quad (2.61)$$

The regularity is enough to ensure the uniform and the improved error bounds in L^2 -norm. The ‘exact’ solution $\psi(x, t)$ is obtained numerically by the TSFP (2.9) with a very fine mesh size $h_\varepsilon = 1/128$ and time step size $\tau_\varepsilon = 10^{-4}$. To quantify the error, we introduce the following error functions:

$$e_{L^2}(t_n) = \|\psi(x, t_n) - I_N\psi^n\|_{L^2}, \quad e_{H^1}(t_n) = \|\psi(x, t_n) - I_N\psi^n\|_{H^1}, \quad (2.62)$$

and

$$e_{L^2, \max}(t_n) = \max_{0 \leq q \leq n} e_{L^2}(t_q), \quad e_{H^1, \max}(t_n) = \max_{0 \leq q \leq n} e_{H^1}(t_q).$$

In the rest of the paper, the spatial mesh size is always chosen sufficiently small and thus spatial errors can be ignored when considering the long time error growth and/or the temporal errors.

Fig. 1 plots the long-time errors in L^2 -norm of the TSFP method for the Schrödinger equation (2.1) with $\varepsilon = 1$ and different time step τ , which shows that the uniform errors in L^2 -norm linearly grows with respect to the time. In addition, for a given accuracy bound, the time to exceed the error bar is quadruple when the time step is half, which also confirms the linear growth. For comparisons, Fig. 2 depicts the long-time errors in L^2 -norm of the fourth-order time-splitting method, respectively, which indicates that higher order time-splitting methods could get

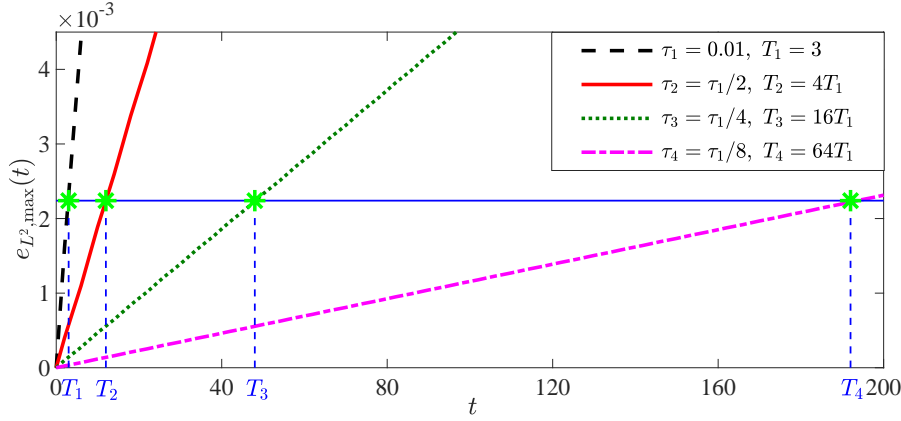


Fig. 1 Long-time temporal errors in L^2 -norm of the TSFP (2.9) for the Schrödinger equation (2.1) with $\varepsilon = 1$ and different time step τ .

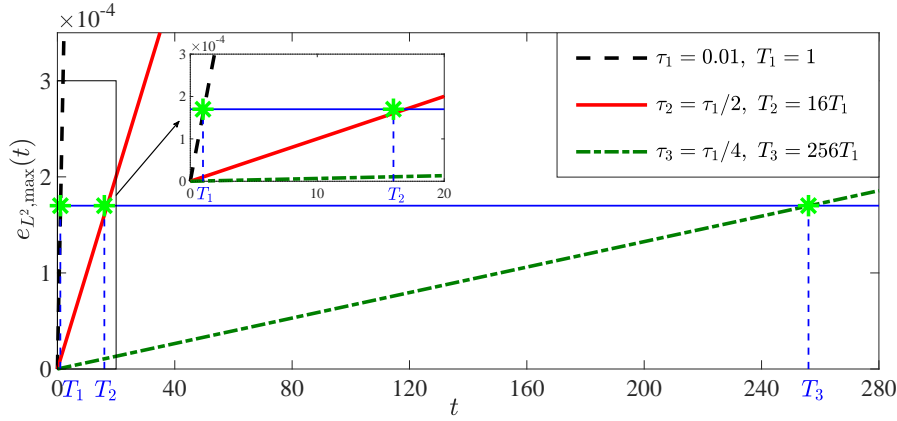


Fig. 2 Long-time temporal errors in L^2 -norm of the fourth-order time-splitting method for the Schrödinger equation (2.1) with $\varepsilon = 1$ and different time step τ .

better accuracy with the same time step size as well as longer time simulations within a given accuracy bound.

Next, we report the convergence test for the Schrödinger equation (2.1) with the potential $V(x) = \sin(x)$ and the smooth initial data

$$\psi_0(x) = 2/(2 + \sin^2(x)), \quad x \in [0, 2\pi]. \quad (2.63)$$

The ‘exact’ solution $\psi(x, t)$ is obtained numerically by the TSFP (2.9) with $h_e = \pi/64$ and $\tau_e = 10^{-4}$.

Fig. 3 displays the long-time errors in H^1 -norm of the TSFP method for the Schrödinger equation (2.1) with the fixed time step τ and different ε , which confirms the improved uniform error bound in H^1 -norm at $O(\varepsilon\tau^2)$ up to the $O(1/\varepsilon)$ time. Figs. 4 & 5 exhibit the spatial and temporal errors of the TSFP (2.9) for the Schrödinger equation (2.1) at $t = \frac{2}{\varepsilon}$. Each line in Fig. 4 (a) shows the spectral accuracy of the TSFP method in space and Fig. 4 (b) verifies the spatial errors

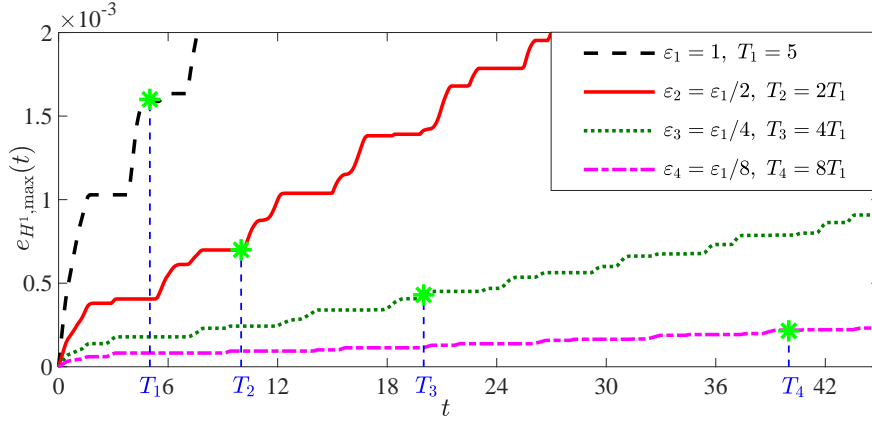


Fig. 3 Long-time temporal errors in H^1 -norm of the TSFP (2.9) for the Schrödinger equation (2.1) with different ε .

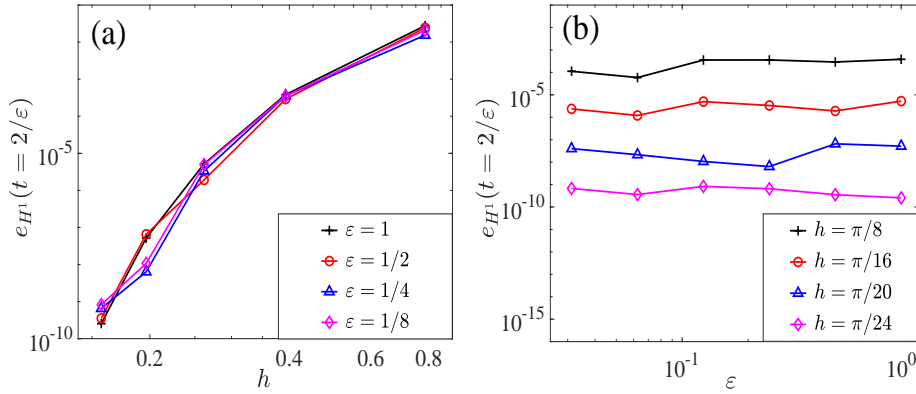


Fig. 4 Long-time spatial errors in H^1 -norm of the TSFP (2.9) for the Schrödinger equation (2.1) at $t = 2/\varepsilon$.

are independent of the small parameter ε in the long-time regime. Fig. 5 (a) shows the second-order convergence of the TSFP method in time. Each line in Fig. 5 (b) gives the global errors in H^1 -norm with a fixed time step τ and verifies that the global error performs like $O(\varepsilon\tau^2)$ up to the $O(1/\varepsilon)$ time.

3 Improved uniform error bounds for the NLSE

In this section, we adopt the TSFP method to solve the NLSE with weak nonlinearity and extend the technique of regularity compensation oscillation (RCO) to obtain improved uniform error bounds for the cubic NLSE with $O(\varepsilon^2)$ -nonlinearity up to the $O(1/\varepsilon^2)$ time.

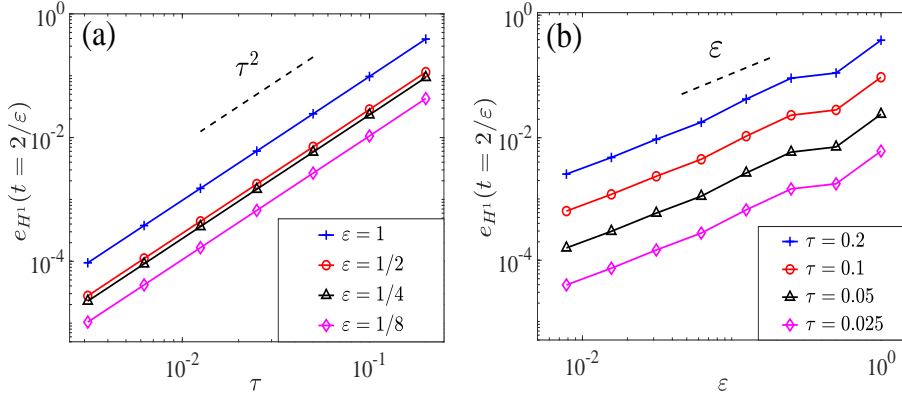


Fig. 5 Long-time temporal errors in H^1 -norm of the TSFP (2.9) for the Schrödinger equation (2.1) at $t = 2/\varepsilon$.

3.1 The TSFP method

We present the TSFP method for the NLSE (1.2) in 1D and extensions to higher dimensions are straightforward (see also Remark 2.5). In 1D, the NLSE (1.2) with initial data (1.3) and periodic boundary conditions on $\Omega = (a, b)$ collapses to

$$\begin{cases} i\partial_t \psi(x, t) = -\Delta \psi(x, t) \pm \varepsilon^2 |\psi(x, t)|^2 \psi(x, t), & a < x < b, t > 0, \\ \psi(a, t) = \psi(b, t), \partial_x \psi(a, t) = \partial_x \psi(b, t), & t \geq 0, \\ \psi(x, 0) = \psi_0(x), & x \in [a, b]. \end{cases} \quad (3.1)$$

By the same time-splitting technique as that in the linear case, the semi-discretization of the NLSE (3.1) via the Strang splitting is given as:

$$\psi^{[n+1]}(x) = \mathcal{S}_\tau(\psi^{[n]}) = e^{i\frac{\tau}{2}\Delta} e^{\mp i\varepsilon^2 \tau} \left| e^{i\frac{\tau}{2}\Delta} \psi^{[n]}(x) \right|^2 e^{i\frac{\tau}{2}\Delta} \psi^{[n]}(x), \quad x \in \Omega, \quad (3.2)$$

with $\psi^{[0]}(x) = \psi_0(x)$. Respectively, the full-discretization for the NLSE (3.1) can be written as

$$\begin{aligned} \psi_j^{(1)} &= \sum_{l \in \mathcal{T}_N} e^{-i\frac{\tau\mu_l^2}{2}} \left(\widetilde{\psi}^{[n]} \right)_l e^{i\mu_l(x_j - a)}, \\ \psi_j^{(2)} &= e^{\mp i\varepsilon^2 \tau \lambda |\psi_j^{(1)}|^2} \psi_j^{(1)}, \quad j \in \mathcal{T}_N^0, \quad n \geq 0, \\ \psi_j^{n+1} &= \sum_{l \in \mathcal{T}_N} e^{-i\frac{\tau\mu_l^2}{2}} \left(\widetilde{\psi}^{(2)} \right)_l e^{i\mu_l(x_j - a)}, \end{aligned} \quad (3.3)$$

where $\psi_j^0 = \psi_0(x_j)$ for $j \in \mathcal{T}_N^0$.

3.2 Improved uniform error bounds in H^1 -norm

For the NLSE, we assume the exact solution $\psi(x, t)$ up to the time at $T_\varepsilon = T/\varepsilon^2$ with $T > 0$ fixed satisfies:

$$(C) \quad \|\psi(x, t)\|_{L^\infty([0, T_\varepsilon]; H_{\text{per}}^m)} \lesssim 1, \quad \|\partial_t \psi(x, t)\|_{L^\infty([0, T_\varepsilon]; H_{\text{per}}^{m-2})} \lesssim 1, \quad m \geq 5.$$

Then we have the following improved uniform error bound of the TSFP (3.3) for the NLSE with $O(\varepsilon^2)$ -nonlinearity strength up to the time at $O(1/\varepsilon^2)$.

Theorem 3.1 *Let ψ^n be the numerical approximation obtained from the TSFP (3.3). Under the assumption (C), there exist $h_0 > 0$, $0 < \tau_0 < 1$ sufficiently small and independent of ε such that, for any $0 < \varepsilon \leq 1$, when $0 < h < h_0$ and $0 < \tau \leq \alpha \frac{\tau_0^2(b-a)^2}{4\pi(1+\tau_0)^2} < 1$ with a constant $\alpha \in (0, 1)$, the following error bounds hold*

$$\begin{aligned} \|\psi(x, t_n) - I_N \psi^n\|_{H^1} &\lesssim h^{m-1} + \varepsilon^2 \tau^2 + \tau_0^{m-1}, \\ \|I_N \psi^n\|_{H^1} &\leq 1 + M, \quad 0 \leq n \leq \frac{T/\varepsilon^2}{\tau}, \end{aligned} \quad (3.4)$$

where $M := \|\psi\|_{L^\infty([0, T_\varepsilon]; H^1)}$. In particular, if the exact solution is sufficiently smooth (e.g. $\psi(x, t) \in H_{\text{per}}^\infty$) and τ_0 is small, the τ_0^{m-1} error part will be extremely small and can be ignored, and the estimate would practically become

$$\|\psi(x, t_n) - I_N \psi^n\|_{H^1} \lesssim h^{m-1} + \varepsilon^2 \tau^2. \quad (3.5)$$

Some parts of the proof proceed in analogous lines as the linear case and we omit the details in this section for brevity. Similar to the analysis of the local truncation error for the linear case, we have the following results for the local truncation error for the TSFP (3.3).

Lemma 3.1 *The local truncation error of the TSFP method (3.3) for the NLSE with $O(\varepsilon^2)$ -nonlinearity strength can be written as ($0 \leq n \leq \frac{T/\varepsilon^2}{\tau} - 1$)*

$$\bar{\mathcal{E}}^n := P_N \mathcal{S}_\tau(P_N \psi(t_n)) - P_N \psi(t_{n+1}) = P_N \mathcal{J}(P_N \psi(t_n)) + Y_n, \quad (3.6)$$

where

$$\mathcal{J}(P_N \psi(t_n)) = -i\varepsilon^2 \tau g\left(\frac{\tau}{2}\right) + i\varepsilon^2 \int_0^\tau g(s) ds, \quad (3.7)$$

with

$$g(s) = \pm e^{i(\tau-s)\Delta} |P_N(\psi(t_n + s))|^2 e^{is\Delta} P_N \psi(t_n). \quad (3.8)$$

Under the assumption (D), for $0 < \varepsilon \leq 1$, we have the error bounds

$$\|\mathcal{J}(P_N \psi(t_n))\|_{H^1} \lesssim \varepsilon^2 \tau^3 \|\psi(t_n)\|_{H^5}^3, \quad \|Y_n\|_{H^1} \lesssim \varepsilon^4 \tau^3 + \varepsilon^2 \tau h^{m-1}. \quad (3.9)$$

Proof for Theorem 3.1. We apply a standard induction argument for proving (3.4). Since $\psi_j^0 = \psi_0(x_j)$, it is obvious for $n = 0$. Assuming the error bounds (3.4) hold true for all $0 \leq n \leq q \leq \frac{T/\varepsilon^2}{\tau} - 1$, we are going to prove the case $n = q + 1$. By Fourier projections $\|\psi(x, t_n) - I_N \psi^n\|_{H^1} \lesssim \|P_N \psi(x, t_n) - I_N \psi^n\|_{H^1} + h^{m-1}$, we just need to analyze the growth of the error $e^n = I^n \psi^n - P_N \psi(t_n)$ carefully. For $0 \leq n \leq q$, we have

$$e^{n+1} = I_N \psi^{n+1} - \mathcal{S}_\tau(P_N \psi(t_n)) + \bar{\mathcal{E}}^n = e^{i\tau\Delta} e^n + Z^n(x) + \bar{\mathcal{E}}^n, \quad (3.10)$$

where $Z^n(x)$ is given by

$$Z^n(x) = e^{i\frac{\tau}{2}\Delta} \left[I_N \left((e^{-i\varepsilon^2\tau\lambda|e^{i\frac{\tau}{2}\Delta} I_N \psi^n|^2} - 1) e^{i\frac{\tau}{2}\Delta} I_N \psi^n \right) - P_N \left((e^{-i\varepsilon^2\tau\lambda|e^{i\frac{\tau}{2}\Delta} P_N \psi(t_n)|^2} - 1) e^{i\frac{\tau}{2}\Delta} P_N \psi(t_n) \right) \right],$$

with the bound (constant in front of $\|e^n\|_{H^1}$ depends on M)

$$\|Z^n(x)\|_{H^1} \lesssim \varepsilon^2 \tau \left(h^{m-1} + \|e^n\|_{H^1} \right). \quad (3.11)$$

From (3.10), we obtain for $0 \leq n \leq q$,

$$e^{n+1} = e^{i(n+1)\tau\Delta} e^0 + \sum_{k=0}^n e^{i(n-k)\tau\Delta} \left(Z^k(x) + \bar{\mathcal{E}}^k \right). \quad (3.12)$$

Similar to the linear case, we get for $0 \leq n \leq q$,

$$\begin{aligned} \|e^{n+1}\|_{H^1} &\lesssim h^{m-1} + \varepsilon^2 \tau^2 + \varepsilon^2 \tau \sum_{k=0}^n \|e^k\|_{H^1} \\ &\quad + \left\| \sum_{k=0}^n e^{i(n-k)\tau\Delta} P_N \mathcal{J}(P_N \psi(t_k)) \right\|_{H^1}. \end{aligned} \quad (3.13)$$

Recalling (3.7) and (3.8), we could decompose $\mathcal{J}(\psi(t_n))$ as

$$\mathcal{J}(P_N \psi(t_n)) = \mathcal{J}_1(P_N \psi(t_n)) + \mathcal{J}_2(P_N \psi(t_n)), \quad (3.14)$$

where $\mathcal{J}_\sigma(P_N \psi(t_n)) = -i\varepsilon^2 \tau g_\sigma(\tau/2) + i\varepsilon^2 \int_0^\tau g_\sigma(s) ds$, $\sigma = 1, 2$ and $g_\sigma(s) := g_\sigma(s; P_N \psi(t_n))$ ($\sigma = 1, 2$) are defined as

$$g_1(s) = \pm e^{i(\tau-s)\Delta} |e^{is\Delta} P_N \psi(t_n)|^2 e^{is\Delta} P_N \psi(t_n), \quad g_2(s) = g(s) - g_1(s),$$

with $g(s)$ ($s \in [0, \tau]$) given in (3.8). Under the assumption (D), by the Duhamel's principle, it is easy to verify $\| |e^{is\Delta} P_N \psi(t_n)|^2 - |P_N \psi(t_n + s)|^2 \|_{L^\infty([0, \tau]; H^m)} \lesssim \varepsilon^2 \tau$. Following similar analysis for the local truncation error in Section 2, for $0 \leq n \leq \frac{T/\varepsilon^2}{\tau} - 1$, we could arrive at

$$\|\mathcal{J}_1(P_N \psi(t_n))\|_{H^1} \lesssim \varepsilon^2 \tau^3, \quad \|\mathcal{J}_2(P_N \psi(t_n))\|_{H^1} \lesssim \varepsilon^4 \tau^3. \quad (3.15)$$

In light of (3.13), we find the major part of the error is from $\mathcal{J}_1(\psi_n)$.

Following the RCO approach in the linear case, we introduce the 'twisted variable' $\phi(x, t) = e^{-it\Delta} \psi(x, t)$, and $\|\partial_t \phi\|_{L^\infty([0, T/\varepsilon^2]; H^m)} \lesssim \varepsilon^2$ with

$$\|\phi(t_n) - \phi(t_{n-1})\|_{H^m} \lesssim \varepsilon^2 \tau, \quad 1 \leq n \leq T/\varepsilon^2. \quad (3.16)$$

We choose the same cut-off parameter $\tau_0 \in (0, 1)$ and the corresponding Fourier modes $N_0 = 2\lceil 1/\tau_0 \rceil$ as in the proof of Theorem 2.2. Thus, we can derive

$$\left\| e^{n+1} \right\|_{H^1} \lesssim h^{m-1} + \tau_0^{m-1} + \varepsilon^2 \tau^2 + \varepsilon^2 \tau \sum_{k=0}^n \left\| e^k \right\|_{H^1} + \|\mathcal{L}^n\|_{H^1}, \quad (3.17)$$

$$\mathcal{L}^n(x) = \sum_{k=0}^n e^{-i(k+1)\tau\Delta} P_{N_0} \mathcal{J}_1(e^{it_k\Delta} (P_{N_0} \phi(t_k))). \quad (3.18)$$

For $l \in \mathcal{T}_{N_0}$, we define the index set $\mathcal{I}_l^{N_0}$ associated to l as

$$\mathcal{I}_l^{N_0} = \{(l_1, l_2, l_3) \mid l_1 - l_2 + l_3 = l, l_1, l_2, l_3 \in \mathcal{T}_{N_0}\}. \quad (3.19)$$

Then, the expansion below follows

$$e^{-i(k+1)\tau\Delta} P_{N_0} \mathcal{J}_1(e^{it_k\Delta} (P_{N_0} \phi(t_k))) = \sum_{l \in \mathcal{T}_{N_1}} \sum_{(l_1, l_2, l_3) \in \mathcal{I}_l^{N_1}} \mathcal{G}_{k, l, l_1, l_2, l_3}(s) e^{i\mu_l(x-a)},$$

where the coefficients $\mathcal{G}_{k, l, l_1, l_2, l_3}(s)$ are functions of s only,

$$\mathcal{G}_{k, l, l_1, l_2, l_3}(s) = e^{i(t_k+s)\delta_{l, l_1, l_2, l_3}} \left(\widehat{\phi}_{l_2}(t_k) \right)^* \widehat{\phi}_{l_1}(t_k) \widehat{\phi}_{l_3}(t_k), \quad (3.20)$$

and $\delta_{l, l_1, l_2, l_3} = \delta_l - \delta_{l_1} + \delta_{l_2} - \delta_{l_3}$ ($\delta_l = \mu_l^2$ as in (3.20)). The remainder term in (3.13) reads

$$\mathcal{L}^n(x) = \pm i\varepsilon^2 \sum_{k=0}^n \sum_{l \in \mathcal{T}_{N_1}} \sum_{(l_1, l_2, l_3) \in \mathcal{I}_l^{N_1}} \Lambda_{k, l, l_1, l_2, l_3} e^{i\mu_l(x-a)}, \quad (3.21)$$

where

$$\begin{aligned} \Lambda_{k, l, l_1, l_2, l_3} &= -\tau \mathcal{G}_{k, l, l_1, l_2, l_3}(\tau/2) + \int_0^\tau \mathcal{G}_{k, l, l_1, l_2, l_3}(s) ds \\ &= r_{l, l_1, l_2, l_3} e^{it_k \delta_{l, l_1, l_2, l_3}} c_{k, l, l_1, l_2, l_3} \end{aligned} \quad (3.22)$$

with coefficients c_{k, l, l_1, l_2, l_3} and r_{l, l_1, l_2, l_3} given by

$$c_{k, l, l_1, l_2, l_3} = (\widehat{\eta}_{l_2}(t_k))^* \widehat{\eta}_{l_1}(t_k) \widehat{\eta}_{l_3}(t_k), \quad (3.23)$$

$$r_{l, l_1, l_2, l_3} = -\tau e^{i\tau \delta_{l, l_1, l_2, l_3}/2} + \int_0^\tau e^{is\delta_{l, l_1, l_2, l_3}} ds = O\left(\tau^3 (\delta_{l, l_1, l_2, l_3})^2\right). \quad (3.24)$$

Similar to the linear case, we only need consider the case $\delta_{l, l_1, l_2, l_3} \neq 0$, as $r_{l, l_1, l_2, l_3} = 0$ if $\delta_{l, l_1, l_2, l_3} = 0$. First, for $l \in \mathcal{T}_{N_0}$ and $(l_1, l_2, l_3) \in \mathcal{I}_l^{N_0}$, we have

$$|\delta_{l, l_1, l_2, l_3}| \leq 2\delta_{N_0/2} = 2\mu_{N_0/2}^2 \leq \frac{8\pi^2(1+\tau_0)^2}{\tau_0^2(b-a)^2}, \quad (3.25)$$

which implies for $0 < \tau \leq \alpha \frac{\tau_0^2(b-a)^2}{4\pi(1+\tau_0)^2}$ with $0 < \tau_0, \alpha < 1$,

$$\frac{\tau}{2} |\delta_{l, l_1, l_2, l_3}| \leq \alpha\pi. \quad (3.26)$$

Denoting $S_{n, l, l_1, l_2, l_3} = \sum_{k=0}^n e^{it_k \delta_{l, l_1, l_2, l_3}}$ ($n \geq 0$) and using summation by parts, we find from (3.22) that

$$\begin{aligned} \sum_{k=0}^n \Lambda_{k, l, l_1, l_2, l_3} &= r_{l, l_1, l_2, l_3} \sum_{k=0}^{n-1} S_{k, l, l_1, l_2, l_3} (c_{k, l, l_1, l_2, l_3} - c_{k+1, l, l_1, l_2, l_3}) \\ &\quad + S_{n, l, l_1, l_2, l_3} r_{l, l_1, l_2, l_3} c_{n, l, l_1, l_2, l_3}, \end{aligned} \quad (3.27)$$

and

$$\begin{aligned}
& c_{k,l,l_1,l_2,l_3} - c_{k+1,l,l_1,l_2,l_3} \\
&= (\widehat{\phi}_{l_2}(t_k))^* (\widehat{\phi}_{l_1}(t_k) - \widehat{\phi}_{l_1}(t_{k+1})) \widehat{\phi}_{l_3}(t_k) + (\widehat{\phi}_{l_2}(t_k) - \widehat{\phi}_{l_2}(t_{k+1}))^* \widehat{\phi}_{l_1}(t_{k+1}) \widehat{\phi}_{l_3}(t_k) \\
&\quad + (\widehat{\phi}_{l_2}(t_{k+1}))^* \widehat{\phi}_{l_1}(t_{k+1}) (\widehat{\phi}_{l_3}(t_k) - \widehat{\phi}_{l_3}(t_{k+1})), \tag{3.28}
\end{aligned}$$

where c^* is the complex conjugate of c . For $0 < \tau \leq \alpha \frac{\tau_0^2(b-a)^2}{4\pi(1+\tau_0)^2}$, we know from (3.26) that for $C = \frac{2\alpha}{\sin(\alpha\pi)}$,

$$|S_{n,l,l_1,l_2,l_3}| \leq \frac{1}{|\sin(\tau\delta_{l,l_1,l_2,l_3}/2)|} \leq \frac{C}{\tau|\delta_{l,l_1,l_2,l_3}|}, \quad \forall n \geq 0. \tag{3.29}$$

Combining (3.24), (3.27), (3.28) and (3.29), we have

$$\begin{aligned}
\left| \sum_{k=0}^n \Lambda_{k,l,l_1,l_2,l_3} \right| &\lesssim \tau^2 |\delta_{l,l_1,l_2,l_3}| \sum_{k=0}^{n-1} \left(\left| \widehat{\phi}_{l_1}(t_k) - \widehat{\phi}_{l_1}(t_{k+1}) \right| \left| \widehat{\phi}_{l_2}(t_k) \right| \left| \widehat{\phi}_{l_3}(t_k) \right| \right. \\
&\quad + \left| \widehat{\phi}_{l_1}(t_{k+1}) \right| \left| \widehat{\phi}_{l_2}(t_k) - \widehat{\phi}_{l_2}(t_{k+1}) \right| \left| \widehat{\phi}_{l_3}(t_k) \right| \\
&\quad + \left. \left| \widehat{\phi}_{l_1}(t_{k+1}) \right| \left| \widehat{\phi}_{l_2}(t_{k+1}) \right| \left| \widehat{\phi}_{l_3}(t_k) - \widehat{\phi}_{l_3}(t_{k+1}) \right| \right) \\
&\quad + \tau^2 |\delta_{l,l_1,l_2,l_3}| \left| \widehat{\phi}_{l_1}(t_n) \right| \left| \widehat{\phi}_{l_2}(t_n) \right| \left| \widehat{\phi}_{l_3}(t_n) \right|. \tag{3.30}
\end{aligned}$$

For $l \in \mathcal{T}_{N_0}$ and $(l_1, l_2, l_3) \in \mathcal{I}_l^{N_0}$, there holds

$$(1 + |\mu_l|) |\delta_{l,l_1,l_2,l_3}| \leq (1 + |\mu_l|) \left[\left(\sum_{j=1}^3 \mu_{l_j} \right)^2 + \sum_{j=1}^3 \mu_{l_j}^2 \right] \lesssim \prod_{j=1}^3 (1 + \mu_{l_j}^2)^{3/2}. \tag{3.31}$$

Based on (3.21), (3.30) and (3.31), we have from (3.13),

$$\begin{aligned}
& \|\mathcal{L}^n\|_{H^1}^2 \\
&= \varepsilon^4 \sum_{l \in \mathcal{T}_{N_0}} \left(1 + \mu_l^2\right) \left| \sum_{(l_1,l_2,l_3) \in \mathcal{I}_l^{N_0}} \sum_{k=0}^n \lambda_{k,l,l_1,l_2,l_3} \right|^2 \tag{3.32} \\
&\lesssim \varepsilon^4 \tau^4 \left\{ \sum_{l \in \mathcal{T}_{N_0}} \left(\sum_{(l_1,l_2,l_3) \in \mathcal{I}_l^{N_0}} \left| \widehat{\phi}_{l_1}(t_n) \right| \left| \widehat{\phi}_{l_2}(t_n) \right| \left| \widehat{\phi}_{l_3}(t_n) \right| \prod_{j=1}^3 (1 + \mu_{l_j}^2)^{\frac{3}{2}} \right)^2 + n \sum_{k=0}^{n-1} \right. \\
&\quad \sum_{l \in \mathcal{T}_{N_0}} \left[\left(\sum_{(l_1,l_2,l_3) \in \mathcal{I}_l^{N_0}} \left| \widehat{\phi}_{l_1}(t_k) - \widehat{\phi}_{l_1}(t_{k+1}) \right| \left| \widehat{\phi}_{l_2}(t_k) \right| \left| \widehat{\phi}_{l_3}(t_k) \right| \prod_{j=1}^3 (1 + \mu_{l_j}^2)^{\frac{3}{2}} \right)^2 \right. \\
&\quad + \left(\sum_{(l_1,l_2,l_3) \in \mathcal{I}_l^{N_0}} \left| \widehat{\phi}_{l_1}(t_{k+1}) \right| \left| \widehat{\phi}_{l_2}(t_k) - \widehat{\phi}_{l_2}(t_{k+1}) \right| \left| \widehat{\phi}_{l_3}(t_k) \right| \prod_{j=1}^3 (1 + \mu_{l_j}^2)^{\frac{3}{2}} \right)^2 \\
&\quad + \left. \left. \left(\sum_{(l_1,l_2,l_3) \in \mathcal{I}_l^{N_0}} \left| \widehat{\phi}_{l_1}(t_{k+1}) \right| \left| \widehat{\phi}_{l_2}(t_{k+1}) \right| \left| \widehat{\phi}_{l_3}(t_k) - \widehat{\phi}_{l_3}(t_{k+1}) \right| \prod_{j=1}^3 (1 + \mu_{l_j}^2)^{\frac{3}{2}} \right)^2 \right] \right\}.
\end{aligned}$$

Introducing the auxiliary function $\xi(x) = \sum_{l \in \mathbb{Z}} (1 + \mu_l^2)^{\frac{3}{2}} |\widehat{\phi}_l(t_n)| e^{i\mu_l(x-a)}$, where $\xi(x) \in H_{\text{per}}^{m-3}(\Omega)$ implied by assumption (D) and $\|\xi\|_{H^s} \lesssim \|\psi(t_n)\|_{H^{s+3}}$. Expanding $|\xi(x)|^2 \xi(x) = \sum_{l \in \mathbb{Z}} \sum_{l_1 - l_2 + l_3 = l} \prod_{j=1}^3 \left((1 + \mu_{l_j}^2)^2 |\widehat{\phi}_{l_j}(t_n)| \right) e^{i\mu_l(x-a)}$, we could obtain that

$$\begin{aligned} & \sum_{l \in \mathcal{T}_{N_0}} \left(\sum_{(l_1, l_2, l_3) \in \mathcal{I}_l^{N_0}} |\widehat{\phi}_{l_1}(t_n)| |\widehat{\phi}_{l_2}(t_n)| |\widehat{\phi}_{l_3}(t_n)| \prod_{j=1}^3 (1 + \mu_{l_j}^2)^{\frac{3}{2}} \right)^2 \\ & \leq \left\| |\xi(x)|^2 \xi(x) \right\|_{L^2}^2 \lesssim \|\xi(x)\|_{H^1}^6 \lesssim \|\psi(t_k)\|_{H^4}^6 \lesssim 1. \end{aligned} \quad (3.33)$$

Noticing (3.16), we can estimate each terms in (3.32) accordingly as

$$\begin{aligned} & \left\| \sum_{k=0}^n e^{-i(k+1)\tau\Delta} P_{N_0} \mathcal{J}_1(e^{it_k\Delta}(P_{N_0}\phi(t_k))) \right\|_{H^1}^2 \\ & \lesssim \varepsilon^4 \tau^4 \left[\|\phi(t_k)\|_{H^4}^6 + n \sum_{k=0}^{n-1} \|\phi(t_k) - \phi(t_{k+1})\|_{H^4}^2 (\|\phi(t_k)\|_{H^4} + \|\phi(t_{k+1})\|_{H^4})^4 \right] \\ & \lesssim \varepsilon^4 \tau^4 + n^2 \varepsilon^4 \tau^4 (\varepsilon^2 \tau)^2 \lesssim \varepsilon^4 \tau^4, \quad n \leq q, \end{aligned} \quad (3.34)$$

and (3.17) implies

$$\|e^{n+1}\|_{H^1} \lesssim h^{m-1} + \tau_0^{m-1} + \varepsilon^2 \tau^2 + \varepsilon^2 \tau \sum_{k=0}^n \|e^k\|_{H^1}, \quad 0 \leq n \leq q. \quad (3.35)$$

Using discrete Gronwall's inequality, we have

$$\|e^{p+1}\|_{H^1} \lesssim h^{m-1} + \varepsilon^2 \tau^2 + \tau_0^{m-1}, \quad 0 \leq q \leq \frac{T/\varepsilon^2}{\tau} - 1, \quad (3.36)$$

which implies the first inequality in (3.4) at $n = q + 1$. There exists $h_0 > 0$, when $h \leq h_0$ and $0 < \tau \leq \tau_0$ with τ_0 sufficiently small, the triangle inequality yields that

$$\left\| I_N \psi^{q+1} \right\|_{H^1} \leq \|\psi(x, t_{q+1})\|_{H^1} + \left\| e^{q+1} \right\|_{H^1} \leq M + 1, \quad 0 \leq q \leq \frac{T/\varepsilon^2}{\tau} - 1, \quad (3.37)$$

which means that the induction process for (3.4) is completed. \square

Remark 3.1 The improved uniform error bound for the NLSE in Theorem 3.1 is for the cubic nonlinearity without the external potential. It is straightforward to extend to the NLSE with the general nonlinearity $\varepsilon^{2p}|u|^{2p}u$ ($p \in \mathbb{Z}^+$) and the external potential $\varepsilon^{2p}V(x)$. The long-time dynamics of the NLSE with $O(\varepsilon^{2p})$ -nonlinearity and $O(1)$ -initial data is equivalent to the NLSE with $O(1)$ -nonlinearity and $O(\varepsilon)$ -initial data. The amplitude of the potential is also $O(\varepsilon^{2p})$, where the scaling is to be consistent with the life-span of the NLSE. The improved H^1 -error bound of the TSFP method for the NLSE with $\varepsilon^{2p}|u|^{2p}u$ nonlinearity up to the time at $O(1/\varepsilon^{2p})$ is $O(h^{m-1} + \varepsilon^{2p}\tau^2 + \tau_0^{m-1})$.

3.3 Numerical results

In this subsection, we present some numerical examples for the NLSE with $O(\varepsilon^2)$ -nonlinearity in 1D and 2D to confirm the improved uniform error bound in H^1 -norm.

First, we show the spatial and temporal errors of the TSFP (3.3) for the NLSE (3.1) on 1D domain $[0, 2\pi]$. The initial data is chosen as

$$\psi_0(x) = 2/(2 + \sin^2(x)), \quad x \in [0, 2\pi]. \quad (3.38)$$

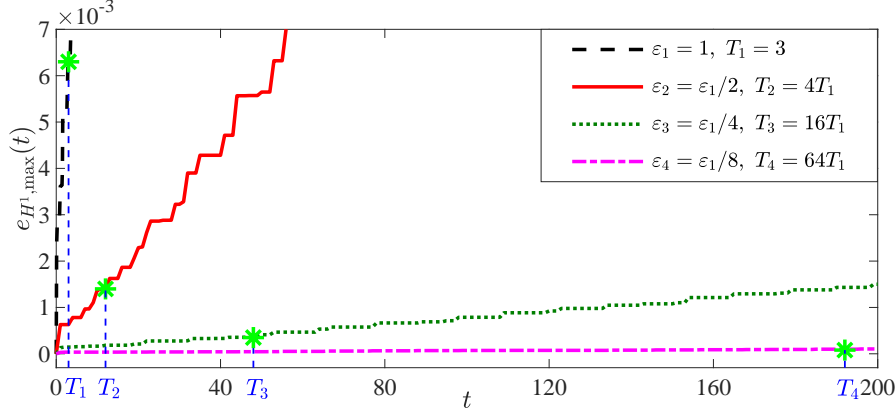


Fig. 6 Long-time temporal errors in H^1 - norm of the TSFP (3.3) for the NLSE (3.1) with different ε .

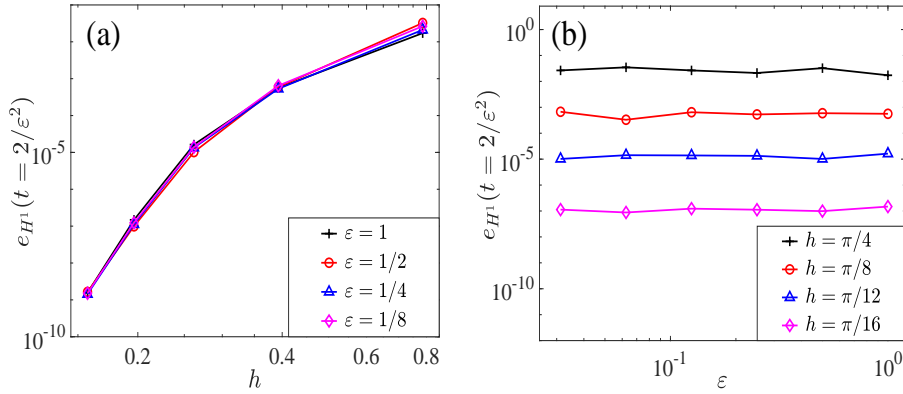


Fig. 7 Long-time spatial errors in H^1 -norm of the TSFP (3.3) for the NLSE in (3.1) with $\lambda = 1$ at $t = 2/\varepsilon^2$.

Fig. 6 plots the long-time errors in H^1 -norm of the TSFP method for the NLSE with a fixed time step τ and different ε , which indicates that the global

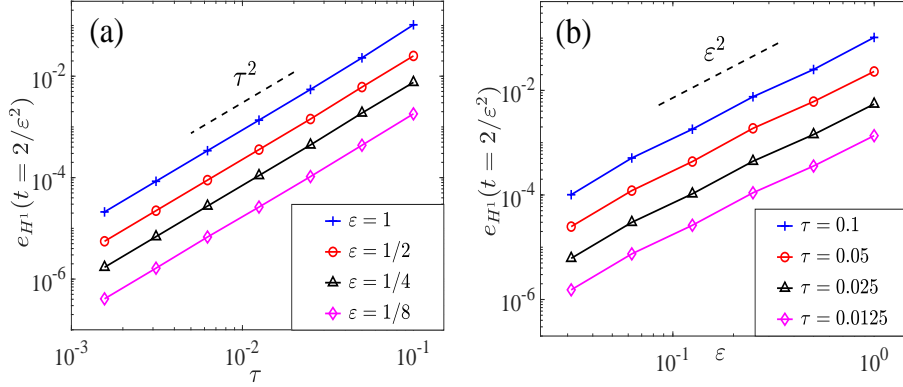


Fig. 8 Long-time temporal errors in H^1 -norm of the TSFP (3.3) for the NLSE (3.1) with $\lambda = 1$ at $t = 2/\epsilon^2$.

errors in H^1 -norm behave like $O(\epsilon^2\tau^2)$ up to the $O(1/\epsilon^2)$ time. Fig. 7 & Fig. 8 depict the long-time spatial and temporal errors of the TSFP (3.3) for the NLSE (3.1) at $t = 2/\epsilon^2$, respectively. Similar to the linear case, Fig. 7 shows the spectral accuracy of the TSFP method for the NLSE in space and the spatial errors are independent of the small parameter ϵ . Each line in Fig. 8 (a) corresponds to a fixed ϵ and shows the global errors in H^1 -norm versus the time step τ , which confirms the second-order convergence of the TSFP method in time. Fig. 8 (b) again validates that the global errors in H^1 -norm behave like $O(\epsilon^2\tau^2)$ up to the $O(1/\epsilon^2)$ time.

Then, we show an example in 2D with the irrational aspect ratio of the domain. We choose the domain $\Omega = (0, \pi) \times (0, 1)$ and the initial data

$$\psi_0(x, y) = \frac{1}{1 + \sin^2(2x)} + \sin(2\pi y), \quad \mathbf{x} = (x, y) \in [0, \pi] \times [0, 1]. \quad (3.39)$$

Fig. 9 plots the long-time temporal errors in H^1 -norm of the TSFP method for the NLSE in 2D with a fixed time step τ and different ϵ , which confirms that the improved uniform error bound in H^1 -norm at $O(\epsilon^2\tau^2)$ up to the $O(1/\epsilon^2)$ time is also suitable for the irrational aspect ratio of the domain. Fig. 10 depicts the long-time errors for the TSFP method for the NLSE in 2D at $t = 1/\epsilon^2$, which again indicates that the TSFP method is second-order in time and validates the improved uniform error bound in H^1 -norm up to the time at $O(1/\epsilon^2)$.

4 Conclusions

Improved uniform error bounds for the time-splitting Fourier pseudospectral (TSFP) methods for the long-time dynamics of the Schrödinger equation with small potential and the nonlinear Schrödinger equation (NLSE) with weak nonlinearity were rigorously established. For the Schrödinger equation with small potential, the linear growth of the uniform error bound in L^2 -norm for the TSFP method was strictly proven with the aid of the unitary property of the solution flow in $L^2(\Omega)$.

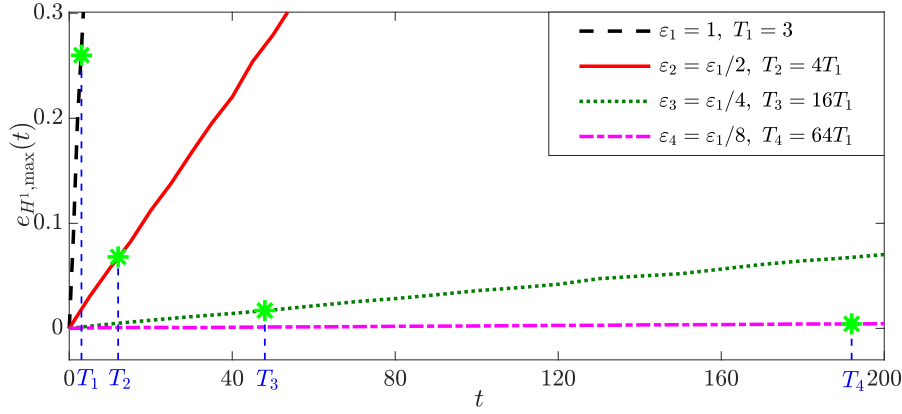


Fig. 9 Long-time temporal errors in H^1 -norm of the TSFP method for the NLSE (1.2) in 2D with different ε .

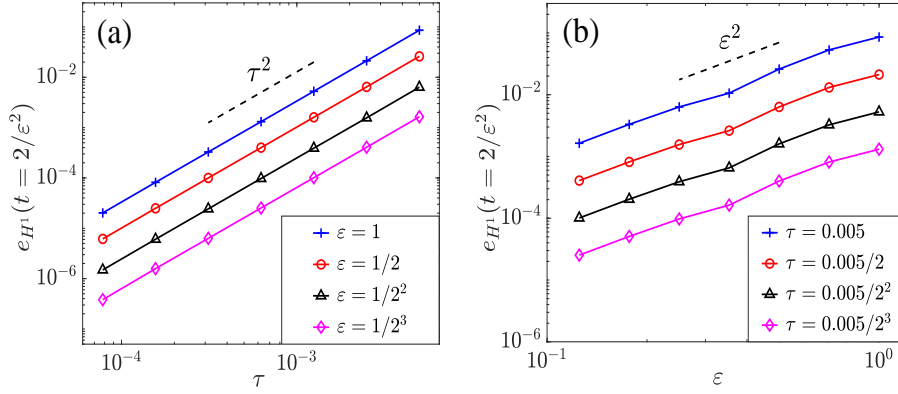


Fig. 10 Long-time temporal errors in H^1 -norm of the TSFP method for the NLSE (1.2) in 2D at $t = 1/\varepsilon^2$.

By introducing a new technique of regularity compensation oscillation (RCO), the improved uniform error bound in H^1 -norm was carried out at $O(h^{m-1} + \varepsilon\tau^2)$ up to the $O(1/\varepsilon)$ time. In addition, the RCO technique was extended to show the improved uniform error bound $O(h^{m-1} + \varepsilon^2\tau^2)$ for the TSFP method applied to the cubic NLSE with $O(\varepsilon^2)$ -nonlinearity up to the $O(1/\varepsilon^2)$ time. Numerical results were presented to validate our error estimates and demonstrate that they are sharp.

Acknowledgement

This work was partially supported by the Ministry of Education of Singapore grant MOE2019-T2-1-063 (R-146-000-296-112, W. Bao, Y. Feng) and NSFC grant 11771036 (Y. Cai).

Conflict of interest

The authors declare that they have no conflict of interest.

References

1. G. D., Akrivis, Finite difference discretization of the cubic Schrödinger equation, *IMA J. Numer. Anal.* 13 (1993), 115–124.
2. X. Antoine, W. Bao, C. Besse, Computational methods for the dynamics of the nonlinear Schrödinger/Gross–Pitaevskii equations, *Comput. Phys. Commun.* 184 (2013), 2621–2633.
3. W. Bao, Y. Cai, Mathematical theory and numerical methods for Bose–Einstein condensation, *Kinet. Relat. Mod.* 6 (2013), 1–135.
4. W. Bao, Y. Cai, Uniform and optimal error estimates of an exponential wave integrator sine pseudospectral method for the nonlinear Schrödinger equation with wave operator, *SIAM J. Numer. Anal.* 52 (2014), 1103–1127.
5. W. Bao, D. Jaksch, P. A. Markowich, Numerical solution of the Gross–Pitaevskii equation for Bose–Einstein condensation, *J. Comput. Phys.* 187 (2003), 318–342.
6. W. Bao, S. Jin, P. A. Markowich, On time-splitting spectral approximations for the Schrödinger equation in the semiclassical regime, *J. Comput. Phys.* 175 (2002), 487–524.
7. W. Bao, J. Shen, A fourth-order time-splitting Laguerre–Hermite pseudospectral method for Bose–Einstein condensates, *SIAM J. Sci. Comput.* 26 (2005), 2010–2028.
8. C. Besse, B. Bidégaray, S. Descombes, Order estimates in time of splitting methods for the nonlinear Schrödinger equation, *SIAM J. Numer. Anal.* 40 (2002), 26–40.
9. J. Bourgain, Fourier transform restriction phenomena for certain lattice subsets and application to nonlinear evolution equations. Part I: Schrödinger equations, *Geom. Funct. Anal.* 3 (1993), 107–156.
10. T. Buckmaster, P. Germain, Z. Hani, J. Shatah, Effective dynamics of the nonlinear Schrödinger equation on large domains, *Comm. Pure Appl. Math.* 71 (2018), 1407–1460.
11. N. Burq, P. Gérard, N. Tzvetkov, Strichartz inequalities and the nonlinear Schrödinger equation on compact manifolds, *Amer. J. Math.* 126 (2004), 569–605.
12. R. Carles, On Fourier time-splitting methods for nonlinear Schrödinger equations in the semiclassical limit, *SIAM J. Numer. Anal.* 51 (2013), 3232–3258.
13. F. Castella, P. Chartier, F. Méhats, A. Murua, Stroboscopic averaging for the nonlinear Schrödinger equation, *Found. Comput. Math.* 15 (2015), 519–559.
14. T. Cazenave, *Semilinear Schrödinger Equations*. Courant Lect. Notes Math., 10, Amer. Math. Soc., Providence, R. I. 2003.
15. E. Celledoni, D. Cohen, B. Owren, Symmetric exponential integrators with an application to the cubic Schrödinger equation, *Found. Comp. Math.* 8 (2008), 303–317.
16. P. Chartier, F. Méhats, M. Thalhammer, Y. Zhang, Improved error estimates for splitting methods applied to highly-oscillatory nonlinear Schrödinger equations, *Math. Comp.* 85 (2016), 2863–2885.
17. W. Chen, X. Li, D. Liang, Energy-conserved splitting FDTD Methods for Maxwell’s equations, *Numer. Math.* 108 (2008), 445–485.
18. W. Chen, X. Li, D. Liang, Energy-conserved splitting finite difference time domain methods for Maxwell’s equations in three dimensions, *SIAM J. Numer. Anal.* 48 (2010), 1530–1554.
19. D. Cohen, E. Hairer, C. Lubich, Modulated Fourier expansions of highly oscillatory differential equations, *Found. Comput. Math.* 3 (2003), 327–345.
20. J. Colliander, M. Keel, G. Staffilani, H. Takaoka, T. Tao, Almost conservation laws and global rough solutions to a nonlinear Schrödinger equation, *Math. Res. Lett.* 9 (2002), 1–24.
21. M. Delfour, M. Fortin, G. Payre, Finite-difference solutions of a nonlinear Schrödinger equation, *J. Comput. Phys.* 44 (1981), 277–288.
22. G. Dujardin, E. Faou, Normal form and long time analysis of splitting schemes for the linear Schrödinger equation with small potential, *Numer. Math.* 106 (2007), 223–262.
23. L. Erdős, B. Schlein, H.-T. Yau, Derivation of the cubic non-linear Schrödinger equation from quantum dynamics of many-body systems, *Invent. Math.* 167 (2007), 515–614.
24. E. Faou, *Geometric Numerical Integration and Schrödinger Equations*. European Mathematical Society, Zürich, 2012.
25. E. Faou, L. Gauckler, Z. Hani, The weakly nonlinear large box limit of the 2D cubic NLS, *J. Amer. Math. Soc.* 29 (2016), 915–982.

26. E. Faou, L. Gauckler, C. Lubich, Sobolev stability of plane wave solutions to the cubic nonlinear Schrödinger equation on a torus, *Comm. Partial Differential Equations* 38 (2013), 1123–1140.
27. E. Faou, B. Grébert, E. Patutel, Birkhoff normal form for splitting methods applied to semilinear Hamiltonian PDEs. I. Finite-dimensional discretization, *Numer. Math.* 114 (2010), 429–458.
28. L. Gauckler, C. Lubich, Nonlinear Schrödinger equations and their spectral semi-discretizations over long times, *Found. Comput. Math.* 10 (2010), 141–169.
29. L. Gauckler, C. Lubich, Splitting integrators for nonlinear Schrödinger equations over long times, *Found. Comput. Math.* 10 (2010), 275–302.
30. E. Hairer, C. Lubich, G. Wanner, *Geometric Numerical Integration: Structure-Preserving Algorithms for Ordinary Differential Equations*. Springer, Berlin, 2002.
31. S. Herr, D. Tataru, N. Tzvetkov, Strichartz estimates for partially periodic solutions to Schrödinger equations in 4d and applications, *J. Reine Angew. Math.* 690 (2014), 65–78.
32. M. Hochbruck, A. Ostermann, Exponential integrators, *Acta Numer.* 19 (2010), 209–286.
33. O. Karakashian, G. D. Akrivis, V. A. Dougalis, On optimal order error estimates for the nonlinear Schrödinger equation, *SIAM J. Numer. Anal.* 30 (1993), 377–400.
34. C. Lubich, On splitting methods for Schrödinger-Poisson and cubic nonlinear Schrödinger equations, *Math. Comp.* 77 (2008), 2141–2153.
35. R. I. McLachlan, G. R. W. Quispel, Splitting methods, *Acta Numer.* 11 (2002), 341–434.
36. J. Shen, T. Tang and L. Wang, *Spectral Methods: Algorithms, Analysis and Applications*, Springer-Verlag Berlin Heidelberg, 2011.
37. G. Strang, On the construction and comparison of difference schemes, *SIAM J. Numer. Anal.* 5 (1968), 506–517.
38. C. Sulem, P. Sulem, *The Nonlinear Schrödinger Equation: Self-Focusing and Wave Collapse*. Springer, New York, 1999.
39. T. Tao, *Nonlinear Dispersive Equations: Local and Global Analysis*. Amer. Math. Soc., Providence RI, 2006.
40. M. Thalhammer, High-order exponential operator splitting methods for time-dependent Schrödinger equations, *SIAM J. Numer. Anal.* 46 (2008), 2022–2038.
41. M. Thalhammer, Convergence analysis of high-order time-splitting pseudospectral methods for nonlinear Schrödinger equations, *SIAM J. Numer. Anal.* 50 (2012), 3231–3258.
42. J. A. C. Weideman, B. M. Herbst, Split-step methods for the solution of the nonlinear Schrödinger equation, *SIAM J. Numer. Anal.* 23 (1986), 485–507.